DR. ESTHER DIANA ROSSI (Orcid ID : 0000-0003-3819-4229)

DR. LIRON PANTANOWITZ (Orcid ID : 0000-0001-8182-5503)

Article type : Review Article

Review article

Cytologic and histological features of rare non-epithelial and non-lymphoid tumors of the thyroid

Esther Diana Rossi MD PhD, MIAC[1], Liron Pantanowitz MD[2] and Jason L. Hornick MD Ph.D [3]

[1]Division of Anatomic Pathology and Histology, Catholic University of Sacred Heart, Rome, Italy; [2] Department of Pathology, University of Michigan, Ann Arbor, MI, USA; [3]Department of Pathology, Brigham and Women's Hospital, Harvard Medical School, Boston, MA, USA

All the authors contributed equally to the paper

***Corresponding author**: Esther Rossi, MD, PhD, MIAC- Division of Anatomic Pathology and Histology – Fondazione Policlinico "Agostino Gemelli"-IRCCS, Università Cattolica del Sacro Cuore,– Largo Francesco Vito, 1 – 00168 Rome (Italy) Phone: +3906-3015-4433; e-mail: esther.rossi@policlinicogemelli.it

RUNNING TITLE: Non-epithelial thyroid tumors

KEY WORDS: Fine needle aspiration cytology, thyroid nodules, non-epithelial tumors, malignancy, rare thyroid entities, sarcoma

Number of pages: 37; Figures: 28; Tables: 3

This is the author manuscript accepted for publication and has undergone full peer review but has not been through the copyediting, typesetting, pagination and proofreading process, which may lead to differences between this version and the Version of Record. Please cite this article as doi: 10.1002/CNCY.22404

Conflict of Interest and Funding.

The authors have no conflict of interest. This work did not receive any specific grant funding.

ABSTRACT

Thyroid tumors can be classified into epithelial, non-epithelial and non-primary lesions. Non-epithelial thyroid tumors are rare. They can be of primary origin within the thyroid gland, arise secondary to contiguous growth from adjacent tissues, or represent metastatic disease. The incidence of these non-epithelial tumors of the thyroid is only 1-2%. Most of these non-epithelial thyroid tumors are lymphomas. The remainder includes mesenchymal and histiocytic tumors. This review examines the cyto-histological features of various non-epithelial and non-lymphoid tumors of the thyroid encompassing vascular lesions, neural tumors including granular cell tumor and paraganglioma, smooth muscle tumors, solitary fibrous tumor, histiocytic neoplasms such as Langerhans cell histiocytosis and Rosai-Dorfman disease, as well as follicular dendritic cell sarcoma. Their differential diagnosis is discussed including recommendations to prevent the pitfall of mistaking these rare tumors for more common epithelial thyroid neoplasms.

1. INTRODUCTON

The majority of thyroid lesions, including benign and malignant entities, are of epithelial origin (1-3). Of the follicular-derived epithelial malignancies, papillary thyroid carcinoma is the most common type of cancer followed by follicular thyroid carcinoma. Medullary thyroid carcinoma arises from parafollicular cells. Non-epithelial malignancies (including lymphoma and mesenchymal lesions, among others) account for only 1-2% of thyroid tumors, the vast majority of which are attributed to different types of lymphoma (3). Nonetheless, the thyroid gland may rarely be involved by other non-epithelial tumors including vascular, neural, smooth muscle, fibroblastic, histiocytic and follicular dendritic cell tumors, as well as teratomas (1, 3-4).

Mesenchymal tumors of the thyroid can present as a solitary nodule or larger mass, or may be identified in a thyroid gland that has been removed for another epithelial lesion. Both benign and malignant mesenchymal tumors of diverse lineages may occur in the thyroid (3-4). Sarcomas represent only a small proportion of primary thyroid malignancies. Virtually all types of sarcoma have been documented manifesting as a primary thyroid malignancy, including osteosarcoma. Among them, angiosarcoma is the most common entity reported in endemic goiter regions of Europe (4-7). Akin to undifferentiated carcinomas of the thyroid gland, these sarcomas tend to occur in older individuals, are rapidly growing and usually fatal due to their local invasiveness.

The cytomorphology of non-epithelial thyroid lesions is identical to that of their counterparts in other body sites. Despite this, it is because of their unusual location in the thyroid that fine needle aspirations (FNA) of these lesions frequently lead to misinterpretation and misdiagnoses (1, 4). The cytological diagnosis of a non-epithelial thyroid tumor can be extremely challenging for cytopathologists. Besides the rarity of these lesions in this anatomic location, several of their morphological features (e.g. papillary structures with fibrovascular cores, granular cytoplasm) may overlap with more typical thyroid epithelial lesions (Table 1). The aim of this review is to explore the

cyto-histological features of various non-epithelial and non-lymphoid tumors that may involve the thyroid gland, highlight the diagnostic role of helpful ancillary studies, and offer recommendations to prevent mistaking these rare tumors for more common epithelial thyroid neoplasms.

2. **VASCULAR LESIONS**

Vascular lesions that may involve the thyroid gland include benign entities such as hemangiomas and malignant lesions such as angiosarcoma (4-19).

2.1 **HEMANGIOMA**

Clinical Findings

Hemangiomas are more likely to be found in the skin and subcutaneous tissue, but have rarely been recorded within the thyroid gland (1-2, 15). The majority of them are clinically obvious and hence not aspirated, unless an FNA is performed to exclude malignancy (15).

Cytopathology

The cytological features are those of an acellular or scant bloody sample, with rare isolated spindle or polygonal cells with moderate cytoplasm and/or tangles/swirls of bland endothelial cells (1,2, 4, 15). (**Figure 1a**)

Histopathology

Hemangiomas are composed of multiple irregular, dilated vessels. These vessels are lined by a monolayer of bland endothelial cells and usually filled with red blood cells. There may be a zone of hemorrhage and atrophy of the adjacent thyroid tissue (15).

Ancillary studies

The cells lining blood vessels are positive for endothelial markers such as CD31, CD34 and ERG. Thyroglobulin and thyroid transcription factor 1 (TTF-1) are negative.

Differential diagnosis

The differential diagnosis includes an organizing thrombus, hematoma or other vascular neoplasm (e.g. epithelioid hemangioendothelioma, Kaposi sarcoma, angiosarcoma). These other vascular lesions are characterized by atypical cellular features.

2.1 **ANGIOSARCOMA**

Clinical Findings

Angiosarcomas are malignant vascular tumors that account for less than 1% of all sarcomas. They arise predominantly in the skin, but also occur in deep soft tissue and viscera including the thyroid gland (6-10, 18). They account for 0.7% of all thyroid cancers (1-4). According to the literature, they occur more often in women, with a peak incidence in the seventh decade (1, 6). Angiosarcoma of the thyroid appears to be more common in the Alpine countries of central Europe where there is a dietary iodine deficiency (2-4). Nonetheless, they have also been documented in countries with adequate iodine intake. Some authors confirmed a significant occupational exposure to vinyl chloride, other polymeric materials and radiation (6-8, 10). In the majority of cases, patients present with a painless mass arising in a long-standing goiter. However, some cases can cause a rapidly growing tumor with compression symptoms. There is a risk of metastases to regional lymph nodes, lung and bone. The majority of thyroid angiosarcomas are of epithelioid type (6-11). Hence, they may exhibit a preponderance of cytological features that resemble carcinoma. For this reason, their cytological diagnosis is challenging.

Cytopathology

FNA smears show variable cellularity ranging from hypocellularity to hypercellular specimens (5, 9, 11-14, 19). The architectural pattern is characterized by single dispersed cells, loose or tight clusters, and focal papillary structures with fibrovascular cores. Individual cells may have a variable appearance ranging from spindled to plasmacytoid or epithelioid with moderate to abundant cytoplasm **(Figures 2a-2b).** Nuclei are typically large, round to oval, and of high nuclear grade, and may have multiple prominent nucleoli (11-13). A necrotic background and mitotic figures are commonly identified on FNA samples. Hemophagocytosis, cytoplasmic vacuoles, and endothelial wrapping may be identified.

Histopathology

These tumors are usually large and have invasive margins (1,2, 18). They may show different morphological patterns including solid, spindled, papillary and pseudopapillary structures composed of irregular gaping vascular channels, although epithelioid cytology is most common (**Figure 2c).** The endothelial cells may show multilayering or a hobnail appearance with projection into the vascular lumen. In solid areas, the cells may have hyaline globules and intracytoplasmic vacuoles Neoplastic cells have abundant eosinophilic cytoplasm, round nuclei with vesicular chromatin, and prominent nucleoli**.** Necrosis and a high mitotic rate are frequently observed.

Ancillary studies

The neoplastic cells are usually strongly and diffusely positive for vascular endothelial markers including CD34, CD31 (**Figure 2d**), and ERG (1, 2, 18). Keratins are variably positive, most often in epithelioid angiosarcomas. Thyroglobulin, TTF-1 and PAX8 are negative (11).

Differential diagnosis

The differential diagnosis varies depending on the angiosarcoma grade. Low-grade angiosarcoma may resemble a hemangioma. High-grade angiosarcoma with solid growth and diverse growth patterns may resemble other poorly differentiated malignancies including anaplastic thyroid carcinoma and other sarcomas (5, 9, 11). Adenomatoid hyperplastic nodules of the thyroid with degenerative and regressive changes might include areas of vascular proliferation. However, these thyroid nodules lack atypia and extensive freely anastomosing vessels. The presence of papillary structures in aspirates from an angiosarcoma, as well an acinar pattern and isolated epithelioid and plasmacytoid cells with cytoplasmic vacuoles that mimic intracellular mucin, may resemble a poorly differentiated adenocarcinoma (1, 6). The diagnosis of angiosarcoma can be confirmed by demonstrating expression of endothelial markers. Also included in the differential diagnosis are metastatic melanoma, epithelioid sarcoma, and plasmablastic lymphoma. A panel of immunostains may be necessary to differentiate these malignancies.

3. **NERVE SHEATH TUMORS**

A nerve sheath tumor is determined to be primary by the fact that the tumor arises within thyroid parenchyma (20-24). Peripheral nerve sheath tumors (PNSTs) of the thyroid account for < 0.02% of all thyroid tumors. The morphological criteria used to diagnose a PNST of the thyroid gland are identical to those used for benign (schwannoma, neurofibroma) and malignant peripheral nerve sheath tumors (MPNST) in other body sites (1-2, 20-32). PNSTs are difficult to diagnose based on clinical findings and sonographic features alone, because they are similar to those of other thyroid entities.

3.1 **SCHWANNOMA AND NEUROFIBROMA**

Clinical findings

Benign PNSTs may occur at any age, but preferentially arise in patients between 40 and 60 years, without any significant gender difference. They usually present as a gradually enlarging mass without specific symptoms and signs. While 25% to 45% of schwannomas occur in the head and neck region, they are extremely rare in the thyroid (1, 2, 20-25). Isolated neurofibromas of the thyroid are also extremely rare (23-24). Neurofibromas may be sporadic or can be seen in the context of neurofibromatosis type 1 (23-24).

Cytopathology

Cytological evaluation for the diagnosis of schwannoma shows low sensitivity, ranging between 0% and 40%, with unsatisfactory specimen rates reported between 36% and 50%. (28-29). The low diagnostic yield with FNA is ascribed to their dense interstitial components, hypocellular Antoni B areas, and frequent cystic degeneration (28), as well as their non-specific cytomorphology (26-27, 31-33). For this reason, some authors have proposed utilizing core needle biopsy (CNB) (30-31). An FNA of a well sampled schwannoma arising in the thyroid shows spindled tumor cells with elongated slender and wavy nuclei, frequently embedded in metachromatic stroma without associated follicular thyroid cells or background colloid (23**). (Figures 3a-3b)**

Neurofibroma on FNA is characterized by fragments of cohesive tissue with a myxoid-fibrillary appearance and mesenchymal tissue with intercellular collagen. Spindle-shaped, widely separated nuclei with pointed ends have been observed (1, 2).

Histopathology

Schwannomas harbor Antoni type A areas characterized by packed, fascicular and focally palisading spindle-shaped cells and Antoni B hypocellular areas with either myxoid, cystic or xanthomatous changes (1-2, 20). The elongated fusiform cells show cytoplasmic extensions giving them a wavy appearance. Nuclei are mostly elongated with occasional degenerative atypia**,** fine chromatin and inconspicuous nucleoli.

Ancillary studies

Schwannomas/neurofibroma are diffusely and strongly positive for S100 protein and SOX10 but are negative for thyroglobulin, chromogranin, smooth muscle actin, muscle-specific actin, desmin, HMB45, Melan-A (1,2, 20). Nevertheless, 63% of the cases are positive for tyrosinase (1,2, 20). S100 protein shows limited expression (or is completely negative) in MPNST (1,2).

Differential diagnosis

Benign PNST are usually accurately diagnosed on H&E alone. A possible differential diagnosis includes some epithelial entities (e.g. medullary carcinoma) and mesenchymal non-neurogenic lesions with spindle features.

3.2 **MALIGNANT PERIPHERAL NERVE SHEATH TUMOR (MPNST)**

Clinical Findings

MPNST is exceptionally rare in children and most often affects older adults (1, 2, 18, 21-22). Malignant transformation of a PNST in the thyroid has been documented, but this is extremely rare (1,2, 20). MPNST are aggressive and invasive tumors, which are frequently associated with a fatal outcome (20, 22).

Cytopathology

FNA of a MPNST is extremely challenging. Cytological smears show highly atypical spindled and/or epithelioid cells without specific features. Wakely et al analyzed 55 cases of MPNST, all with tissue confirmation (33-34). The authors found that the majority of smears were highly cellular, but this was somewhat variable because in a minority of FNAs either fibrosis or abundant blood aspirated with neoplastic cells had a dilutional effect. FNA smears showed single dissociated cells, and syncytial cell clusters of uneven size and cellularity characterized by a 3-dimensional effect leading to the inability to observe cells in the center of these aggregates **(Figures 4a-b).** In some cases, fascicular arrangements within aggregates have been observed. Smear background is mostly clean, but some aspirates may contain strips of collagen or fibrillary metachromatic-staining stroma and scant or lack of a necrotic component. The majority of dispersed cells are uniform in size and shape with oval and/or elongated nuclei with smooth contours and inconsistently tapered or blunt-ended. In some cases, nuclei have a slight "hook" at one pole, producing a so-called comma shape. Lesional cells have finely granular, evenly dispersed nuclear chromatin with small chromocenters; coarsely granular chromatin and macronucleoli are rare findings. As a result, it is often difficult to reach a conclusive and specific diagnosis prior to their surgical management.

Histopathology

Histologically, the majority of cases show a fascicular appearance; distinctive features that may suggest MPNST include alternating cellular and more myxoid areas, and perivascular accentuation or whirling of tumor cells. MPNST has an invasive growth pattern and increased cellularity with fusiform and spindled cells arranged in highly cellular fascicles, sometimes with a herringbone pattern (1, 2, 20) **(Figures 4c)**. A diagnosis of MPNST is based on evidence of cellular pleomorphism with highly atypical nuclei, increased mitotic activity, and necrosis Heterologous differentiation (most often rhabdomyoblastic or chondro-osseous) is observed in 5-10% of cases; very rare cases show glandular differentiation.

Ancillary studies

MPNSTs express S100 protein and SOX10 in only 30-50% of cases. S100 protein immunoreactivity is less extensive than in benign PNSTs. They are uniformly negative for thyroglobulin, keratin, TTF1, chromogranin, calcitonin, Melan-A, HMB45. PAX8 can be positive in 70% of the cases (1, 2, 20). Loss of histone H3K27me3 (histone H3 with lysine 27 trimethylation) by immunohistochemistry is highly specific **(Figure 4d),** but only moderately sensitive for MPNST (35-36).

Differential diagnosis

The differential diagnosis between MPNST and anaplastic thyroid carcinoma with spindle cell features may be difficult and requires the support of immunohistochemistry to confirm lack of all epithelial and thyroid markers in MPNST (1-2). The possibility of a medullary thyroid carcinoma can be excluded based on negativity for calcitonin, CEA and other neuroendocrine markers. Metastatic melanoma can mimic MPNST, especially spindle cellular melanoma. Strong and diffuse S100 protein and SOX10 are not seen in MPNST; positivity for Melan A, HMB-45, tyrosinase and/or MITF can also help support the diagnosis of melanoma, although the sensitivity of these markers in the metastatic setting is only moderate. Other entities in the differential diagnosis to mention are malignant teratomas of the thyroid gland, and metastases. For both of them the combination of morphological features and the evaluation of their immunoprofile are likely to provide useful information for making a cytological diagnosis (34).

4. **PARAGANGLIOMA**

Clinical findings

Paraganglioma of the thyroid is defined as an intrathyroidal neuroendocrine tumor that originates from neural-crest derived paraganglia of the autonomic nervous system (37-40). They likely arise from the inferior laryngeal paraganglia, which can be frequently seen within the thyroid gland instead of adjacent to the larynx (1, 2). Thyroid paraganglioma is an extremely rare thyroid entity, accounting for < 0.01% of all head and neck neoplasms (1, 2, 4). Only 36 cases have been described, mostly on surgical samples (40). There is a slight female predominance and the median age at presentation is around 48 years. The majority of these neoplasms are asymptomatic and occasionally may be discovered during an ultrasound evaluation of the thyroid. Multifocal tumors may be seen in patients with familial paraganglioma-pheochromocytoma syndrome, defined by a mutation in the succinate dehydrogenase subunit genes *SDHD*, *SDHC* or *SDHB* (1,2, 37-45).

Cytopathology

The cytological diagnosis of paraganglioma is challenging and, not surprisingly, might lead to misdiagnoses. FNA smears are cellular and contain single cells or loose clusters of medium-large cells (37, 41-43). The neoplastic cells have epithelioid, plasmacytoid, and spindle features. They have scant to moderate basophilic cytoplasm, round to oval nuclei, open chromatin, and inconspicuous nucleoli **(Figures 5a-5b).** Nuclear overlapping, naked nuclei, nuclear crush artifact and occasional intranuclear pseudoinclusions may be seen in some samples. Occasional pleomorphic cells may be noted, a typical feature of neuroendocrine tumors. The smears are characterized by a bloody background and lack colloid or an amyloid component. Malignancy in paraganglioma cannot be reliably diagnosed on cytological smears (or histology) (41-43).

Histopathology

Paragangliomas are usually well-circumscribed and encapsulated tumors (1, 2). They are highly vascular with cells organized into alveolar, lobular and a Zellballen pattern with delicate fibrous septa **(Figure 5c).** The neoplastic cells are polygonal with abundant granular and amphophilic cytoplasm, and may have occasional vacuoles **(Figure 5d).** These cells have round-to-oval nuclei with coarse chromatin and small nucleoli. Spindled sustentacular cells can be seen at the periphery of the cell nests. They frequently show intratumoral sclerosis and hyalinization. These lesions do not typically have necrosis or mitotic figures.

Ancillary studies

There is a different IHC profile for carotid body versus soft tissue paragangliomas (**43-46**). Specifically, soft tissue paragangliomas show diffuse positivity for synaptophysin (98%) and S100 (80%) and focal positivity for keratins (5%) whilst carotid body paragangliomas have focal positivity for S100 (2%) and negativity for keratin and synaptophysin (44). A paper by Staturwar et al including 5 thyroid paragangliomas documented positivity for synaptophysin, chromogranin, as well as S100 of sustentacular cells, but negative staining for pankeratin, TTF-1, thyroglobulin, calcitonin, CEA and HBME (47). Hence, based on this limited case series the IHC profile of thyroid paragangliomas seems to best match that of soft tissue paragangliomas and not carotid body tumors. Furthermore, paragangliomas are also negative for PAX8. Loss of SDHB is observed in tumors from patients with germline *SDHX* mutations (1, 2, 43-50).

Differential diagnosis

The most important differential diagnoses to consider include hyalinizing trabecular tumor (HTT), papillary thyroid carcinoma (PTC), medullary thyroid carcinoma, intrathyroid parathyroid tumor and

metastases (e.g. melanoma, neuroendocrine tumor). HHT, previously known as "paraganglioma-like adenoma of the thyroid" (PLAT) may resemble a paraganglioma. HHT is characterized by a trabecular pattern, intralesional fibrosis, intranuclear cytoplasmic inclusions, low nuclear/cytoplasm ratio, perinucleolar halos (vacuoles) and yellow bodies. Additionally, HHT cells show positivity for TTF-1, thyroglobulin and have characteristic membranous positivity for MIB-1. With molecular testing, *GLIS* fusions are also highly specific for HTT. PTC has intranuclear inclusions and nuclear grooves that are not typically seen in paraganglioma. PTC shows positivity for thyroid markers. Of note, a paraganglioma-like medullary thyroid carcinoma has been described (50). The presence of intracytoplasmic eosinophilic granules and amyloid are helpful clues for diagnosis of medullary thyroid carcinoma (37-40). Furthermore, medullary thyroid carcinomas show immunopositivity for TTF-1, calcitonin and CEA. Unlike paraganglioma, intrathyroid parathyroid tumors are positive for parathyroid hormone (PTH). Metastatic neuroendocrine tumors to the thyroid gland share similar morphologic features and an immunoprofile with paraganglioma. However, metastatic neuroendocrine tumors tend to be multifocal and demonstrate immunoreactivity for keratins (e.g. AE1/AE3).

5. **GRANULAR CELL TUMOR**

Clinical features

Granular cell tumor (GCT) is an extremely rare primary tumor of the thyroid. With the aid of ultrastructural and immunohistochemical studies they are now confirmed to be of neural (Schwann cell) origin (51). Their most common location is the head and neck, particularly the tongue (1, 2, 51-65). To date, around 20 GCTs arising in the thyroid gland have been described in the literature. Their diagnosis is challenging mostly due to the rarity in this exact anatomic location and because their clinical-radiological findings mimic malignancy (1, 2, 4, 56-63). The majority of reported patients were females with an age range between 20 and 50 years (51-65).

Cytopathology

A GCT in the thyroid can be easily misdiagnosed as follicular neoplasm (60-63). FNA smears are composed of single cells, pseudofollicles, or syncytial clusters of large epithelioid cells characterized by indistinct cell borders and fragile cytoplasm with prominent eosinophilic granules **(Figures 6a-6b).** Tumor cells have bland oval to round or sometimes spindle shaped nuclei with rare and/or inconspicuous nucleoli. One of the most helpful findings is the granular background in smears.

Histopathology

GCTs are composed of sheets or nests with fibrous septa (1, 2). Tumor cells are large, epithelioid and polygonal with abundant granular eosinophilic cytoplasm. Their nuclei are round to oval with regular nuclear membranes, uniform chromatin and inconspicuous nucleoli **(Figure 6c).** Mitotic figures are rare.

Ancillary studies

Their immunoprofile of GCT shows strong positivity for S-100 protein (nuclear and cytoplasmic), SOX10, and calretinin. They are negative for keratins, TTF-1, thyroglobulin, PAX8, calcitonin and chromogranin.

Differential diagnosis

GCT may mimic oncocytic thyroid neoplasms (Hürthle cell adenoma, Hürthle cell carcinoma, oncocytic variant of PTC, and oncocytic variant of MTC) or a paraganglioma (51-60) (Table 3). While Hürthle cell neoplasms are similarly comprised of large epithelioid cells with abundant granular cytoplasmic granules, unlike GCT their cells have well-defined cell borders and lack a granular background. Hürthle cell nuclei also show typical cherry-red nucleoli. Oncocytic metaplasia is often associated with a lymphocytic background. GCT can also mimic macrophages seen with cystic change in thyroid lesions. Macrophages, however, are characterized by foamier cytoplasm and vesicular nuclei, and may have hemosiderin-laden granules. One of the most important diagnoses to be excluded is MTC, which can exhibit a wide cytomorphologic spectrum including spindle and/or oncocytic cells with granular cytoplasm, large nuclei, stippled chromatin, and prominent nucleoli (60-63). Immunopositivity for synaptophysin, chromogranin, CEA and calcitonin will help confirm the diagnosis of MTC.

6. **SMOOTH MUSCLE TUMORS**

Clinical findings

To date, fewer than 50 cases of benign and malignant primary smooth muscle tumors of the thyroid have been reported in the literature (1, 2, 66-76). Primary smooth muscle tumors (SMT) of the thyroid represent <0.02% of all thyroid gland tumors. This extremely rare group of thyroid neoplasms is defined by pathologic criteria similar to those used to diagnose leiomyoma and leiomyosarcoma in other locations (1-2, 66, 71-76). There is no known etiology for most SMTs of the thyroid, other than the rare Epstein-Barr virus-associated tumors associated with AIDS (75). Leiomyomas are more common in younger patients than leiomyosarcomas, which usually affect patients during the sixth and seventh decades. Prevalence for females70-73).

Cytopathology

Cytological specimens from a leiomyoma show a population of monomorphic spindle-shaped cells (67, 73). Tumor cells show slightly hyperchromatic, blunt-ended elongated nuclei, which are usually centrally located. Only case reports of leiomyosarcomas have been published, which reported showing a population of atypical spindle cells with pleomorphic nuclei, mitotic figures, and possible necrosis **(Figure 7).**

Histopathology

Leiomyomas are characterized by intersecting fascicles of bland spindle-shaped smooth muscle cells (1-2, 66, 71). The cells are spindled and blunt-ended (cigar-shaped) with hyperchromatic centrally located nuclei. Leiomyosarcomas show the morphological features of malignant smooth muscle tumors including high cellularity, disordered fascicular growth pattern, and tumor necrosis. Leiomyosarcoma cells are usually characterized by markedly atypical and pleomorphic nuclei as well as mitotic activity.

Ancillary studies

Both leiomyoma and leiomyosarcoma are positive for smooth muscle actin, muscle specific actin, h-caldesmon, and desmin. Thyroglobulin, TTF1, PAX8, calcitonin, chromogranin, and S100 protein are negative.

Differential diagnosis

The differential diagnosis of a smooth muscle tumor will depend on whether it is benign or malignant. Other spindle cell neoplasms to consider in the thyroid are the spindle cell variant of anaplastic carcinoma (ATC), MTC, spindle epithelial tumor with thymus-like differentiation (SETTLE), and other mesenchymal spindle cell neoplasms (Table 2). A panel of immunohistochemical stains can be used to confirm the diagnosis and exclude other entities.

7. SOLITARY FIBROUS TUMOR

Clinical findings

Solitary fibrous tumor (SFT) has been described in several extrapleural sites including the thyroid gland (1-2, 78-80). Regardless of its location, SFT is defined as a fibroblastic tumor composed of spindle cells, showing a characteristic hemangiopericytic vascular pattern associated with *STAT6* rearrangement (1, 2). SFT has an equal sex distribution and presents mostly in patients of middle age. They tend to be slow growing masses.

Cytopathology

The cytological features include paucicellular smears comprised of slender, dyscohesive spindle-shaped cells intermingled with pink, amorphous and collagenized stromal tissue (1, 78-80) **(Figure 8a).** Naked nuclei may be observed in the background. SFT with a high-risk for metastasis often shows more nuclear atypia and mitotic activity. Cases in which a cell-block is available may reveal tumor fragments with a hemangiopericytoma-like architecture.

Histopathology

SFTs are composed of spindle cells with a haphazard distribution ("patternless" pattern) of either nodular or infiltrative architecture within the surrounding thyroid parenchyma (1,2, 18, 78-81). They often have extensive collagen and dilated, thin-walled, branching ("staghorn") vessels **(Figure 8b).** Tumor cells have minimal eosinophilic cytoplasm, nuclei with variable shapes ranging from oval to spindle-shaped, and finely dispersed chromatin with inconspicuous nucleoli. The degree of tumor cellularity is variable. Risk of malignant behavior can be predicted by age, tumor size, mitotic activity, and necrosis (81).

Ancillary studies

SFTs are consistently positive for STAT6 protein, showing nuclear expression which reflects the presence of an *NAB2-STAT6* gene fusion characteristic of these tumors (1, 81). Co-expression of CD34, CD99, and bcl-2 in these tumors has been reported, although these markers lack specificity (83). Neoplastic cells are negative for keratins, actin, desmin, S100 protein, thyroglobulin, TTF-1, PAX8, calcitonin, chromogranin and synaptophysin.

Differential diagnosis

In the thyroid, SFT needs to be distinguished from several entities including MTC, which can often be of spindle cell-type, follicular adenoma with spindle cell features, ectopic thymoma, spindle epithelial tumor with thymus-like differentiation (SETTLE), HTT and other spindle-shaped mesenchymal lesions. Of note, the present of pleomorphic nuclear features, high-grade nuclear morphology may represent clues to help rule out some malignant tumors in the differential diagnosis. Immunohistochemistry is needed to confirm the diagnosis, especially STAT6, which is highly specific for SFT (81). Suster et al studied seven cases of papillary thyroid carcinoma with desmoid-fibromatosis-like and one nodular fasciitis-like stroma (83). All cases had features of conventional papillary thyroid carcinoma embedded in abundant myofibroblastic stroma. The myofibroblastic stroma in six cases resembled desmoid fibromatosis and in one case it more closely resembled nodular

fasciitis. The immunohistochemical staining demonstrated that the stromal spindle component had positivity for SMA and low MIB1 proliferation index in all cases, with patchy strong nuclear positivity for beta-catenin in six out of seven cases (83). Stains for keratins AE1/AE3 and PAX8 were positive in the epithelial elements but negative in the stromal component.

8. **FOLLICULAR DENDRITIC CELL SARCOMA**

Clinical findings

Follicular dendritic cell (FDC) sarcoma is a rare neoplasm that arises from follicular dendritic cells (85-92). FDC sarcomas are mostly nodal in origin, with cervical lymph nodes being the most common site of presentation (1, 2, 4). Involvement of the thyroid gland has been exceptionally reported (85-92). It is more frequently seen in female adult patients showing a slowly growing painless mass without any significant correlation with Hashimoto thyroiditis. In up to 20% of cases, cervical lymph nodes have alterations of the hyaline vascular type of Castleman disease.

Cytopathology

FDC sarcoma is often difficult to diagnose on cytology material alone (85-92). The presence of spindle and epithelioid cells forming a fascicular, syncytial, and/or whorled pattern is often observed. The tumor cells have moderate cytoplasm, round to spindled nuclei, vesicular nuclear chromatin and prominent nucleoli. Lymphocytes are often present.

Histopathology

FDC sarcomas are unencapsulated (1, 2, 4, 85-92). Tumor cells form syncytia, sheets, and fascicles and often show a whorled appearance. The cells may be spindled and/or epithelioid. Their nuclei are round-ovoid, elongated with delicate nuclear membranes, vesicular, have dispersed chromatin and prominent nucleoli (**Figure 9**). The presence of open-vesicular nuclear chromatin, resembling intranuclear inclusions, might be problematic in thyroid cytological samples, leading to a false suspicious for papillary thyroid carcinoma. Some authors report the presence of grape-like clusters of nuclei forming giant cells resembling Warthin-Finkeldey cells (85-92). The mitotic rate is variable.

Ancillary studies

FDC sarcoma neoplastic cells show immunopositivity for CD21, CD35, CD23, D2-40, and clusterin and variable expression of EMA and S100 protein. These cells are negative for keratins (AE1/AE3 and CAM 5.2), actin, desmin, CD34, Calcitonin, PAX8 and CD1a. Griffin et al identified recurrent

loss-of-function alterations in tumor suppressor genes, mutations in genes involved in the negative regulation of NF-κB activation and cell cycle progression (93).

Differential diagnosis

The most important differential diagnosis, due to the often-spindled nature of the cells includes MTC, ATC, SETTLE and other mesenchymal tumors (91). The cytological features combined with the support of immunocytochemistry are extremely helpful in rendering a conclusive diagnosis.

9. **LANGERHANS CELL HISTIOCYTOSIS**

Clinical findings

Langerhans cell histiocytosis (LCH) is associated with three different syndromes that share the same histological features including (i) eosinophilic granuloma, (ii) Hand-Schuller-Christian disease and (iii) Letterer-Siwe disease (1,2, 4). In each of these diseases there are neoplastic cells with the immunophenotype of Langerhans cells, which are derived from the myeloid/monocyte lineage. These cells contain Birbeck granules on electron microscopy. The presence of Langerhans cells in the thyroid can be an isolated phenomenon or part of a systemic disease (90-101). Primary LCH of the thyroid is extremely rare. Afflicted patients range in age from a few months to the elderly, and there is an equal gender distribution (93-100). Young age at presentation is more common with systemic disease, whilst patients of older age more common manifest with isolated involvement of the thyroid (93-98). Prior reported cases were initially diagnosed as thyroid malignancies with lymph node metastasis (99). The final diagnosis in these cases was made histologically only after total thyroidectomy was performed. Of note, some authors reported that LCH occurs in conjunction with PTC (102-104).

Cytopathology

LCH is characterized by cellular smears (92, 100-101, 105-106). There is usually a mixture of large mononuclear or multinucleated histiocytoid cells with nuclear grooves and foamy granular cytoplasm **(Figure 10a),** along with eosinophils and possible Charcot Leyden crystals. FNA samples lack follicular cells and background colloid. Phulware et al described a series of 47 cases of LCH diagnosed on cytological material over a period of 14 years (105). Their findings showed moderate to high cellularity in 58% of cases and abundant Langerhans cells in 72% of them. The presence of giant cells was recognized in 78% of their cases, combined with mild eosinophilia in 61%, sparse lymphocytosis in 83% and mild neutrophilic infiltration in 64% (105). Hang et described similar cytological features concluding that LCH can be accurately diagnosed in FNA based on the

characteristic cytomorphology and selected immunohistochemistry (106). Diagnosis may be difficult in cases with scant or insufficient cellular material (106).

Histopathology

LCH can be either diffuse or focal, and composed of histiocytoid cells with delicate pale or eosinophilic cytoplasm and vesicular nuclei (1, 2, 4, 102-106). Tumor cell nuclei show indented, folded, grooved and often a coffee bean shaped appearance. An increased number of eosinophils have been documented. The infiltrate of Langerhans cells pushes on the surrounding thyroid parenchyma, destroying neighboring follicular structures. A background of Hashimoto thyroiditis is common. (1)

Ancillary studies

Tumor cells in LCH show positivity for S100 protein (nuclear), CD1a (cytoplasm), Langerin (CD207, in Birbeck granules, **Figure 10b**), and CD68. A subset of LCH cases may be immunoreactive for *BRAFV600E*–VE1 antibody. Langerhans cells are negative for keratins, thyroglobulin, TTF-1 and PAX8. Around 50% of LCH have either $BRAF^{V600E}$ or *MAP2K1 (MEK1*) mutations (104-105). Kuhn et al emphasized the critical diagnostic pitfalls due to the use of $BRAF^{V600E}$ mutation analysis in thyroid FNA (104). In fact, $BRAF^{V600E}$ mutation may be found in melanoma, colorectal carcinoma, lung carcinoma, ovarian carcinoma, brain tumors, hairy cell leukemia, plasma cell myeloma, and histiocytosis (107-108).

Differential diagnosis

The most important differential diagnoses include PTC, especially those cystic neoplasms with atypical histiocytoid cells, ATC, and other histiocyte-rich inflammatory conditions or histiocytic disorders. PTC contains malignant follicular cells showing nuclear pseudoinclusions, nuclear grooves and atypical-pleomorphic nuclei. The expression of thyroglobulin and TTF-1 is useful, while $BRAF^{V600E}$ may be seen in both lesions (108). ATC is always composed of cells with severe atypical and pleomorphic features, extensive necrosis, and a different immunoprofile. In Rosai-Dorfman disease, lesional cells are characterized by emperipolesis, which is not seen in LCH.

10. **ROSAI-DORFMAN DISEASE**

Clinical findings

Rosai-Dorfman disease (RDD), also known as sinus histiocytosis with massive lymphadenopathy, is a rare proliferation of distinctive histiocytes that primarily involves lymph nodes (109-116). Thyroid gland involvement is rare and usually occurs in the context of cervical lymph node or systemic

involvement (114-116). Extranodal involvement of RDD has been reported in 43% of cases, mostly in skin, central nervous system and salivary gland locations. Published data shows that RDD occurs mostly in women with a mean age of 56 years (109-116). Thyroid involvement is usually discovered incidentally. Autoimmune disorders (e.g. autoimmune hemolytic anemia, pernicious anemia with gastritis) can be seen in 13% of RDD cases. Gianella et al report that thyroid and tracheal infiltration by RDD can have increased numbers of IgG4-bearing plasma cells (110). RDD and IgG4-related disease share some similar features; differentiation between the two is based on the presence of the distinctive histiocytes and the degree of IgG4-positive infiltrates and IgG4/IgG ratio (110).

Cytopathology

FNA smears show large histiocytes with abundant cytoplasm, indistinct cell borders, emperipolesis, and round vesicular nuclei with distinct central nucleolus (103-105) (**Figures 11a-b).** Intracytoplasmic inflammatory cells include lymphocytes, plasma cells, and neutrophils.

Histopathology

Lesions contain a variable mix of histiocytes as well as lymphocytes, plasma cells and neutrophils (109-116). The neutrophils may be prominent with microabscess formation. The histiocytes are often organized in clusters. These large cells have uniform features including round to oval nuclei, without grooves or nuclear indentations, and vesicular cytoplasm with central nucleoli. The presence of emperipolesis in the cytoplasm of histiocytes is a characteristic finding (**Figure 11c**).

Ancillary studies

The histiocytes are positive for S-100 protein **(Figure 11d)** and CD68 They are negative for CD1a, T-cell antigens, B-cell antigens and Langerin, keratins, TTF1, and PAX8.

Differential diagnosis

The most common differential diagnoses include PTC, ATC, chronic granulomatous inflammation and LCH. PTC shows nuclear atypia which is not evident in RDD samples. Powell et al reported a case of RDD misdiagnosed as ATC, mostly based on the rapid growth of the lesion. Nevertheless, the lack of pleomorphic cells and bizarre nuclei present in a necrotic background, along with immunohistochemistry, can help exclude ATC. Chronic granulomatous inflammation is associated with acute and chronic inflammation as well as epithelioid histiocytes and multinucleated cells, which are not similar to the large pale histiocytes of RDD. LCH typically contains eosinophils, folded nuclei with grooves, and have less cytoplasm than RDD, and lack emperipolesis. LCH also has a different

immunoprofile compared to RDD. Of note, since RDD can have increased levels of IgG4-bearing plasma cells the differential diagnosis includes IgG4-related disease. Nevertheless, the presence of abundant emperipolesis is highly suggestive for RDD and the levels of IgG4-bearing plasma cells insufficient to make a diagnosis of IgG4-related disease. However, the significance of IgG4-bearing plasma cells in RDD remains to be further elucidated, and their presence might indicate a better treatment response to corticosteroids and/or rituximab in case of disease progression (110).

Although emperipolesis is a hallmark feature of RDD, this cellular phenomenon can also occasionally be seen with other hematolymphoid disorders (e.g. lymphoma, leukemia) and tumor cell cannibalism associated with non-hematological malignancies (e.g. poorly differentiated carcinoma).

11 **TERATOMAS**

Clinical findings

Primary thyroid teratomas are exceptionally rare, representing 0.1% of primary thyroid gland neoplasms (1-2). The age of afflicted patients ranges from newborns to elderly patients, with an average age of <10 years. Although more than 90% of thyroid teratomas in neonates are benign, more than 50% of such tumors in adults are malignant (1-2, 118-121). Patients usually present with a neck mass, often accompanied by dyspnea. The ultrasound evaluation commonly shows a multicystic mass in the thyroid. Teratomas show a wide size range, up to 13 cm, and a smooth to bosselated or lobulated outer surface. These tumors are firm to soft and may be cystic. Cystic spaces contain creamy or mucoid material or even hemorrhagic fluid with necrosis. Bone, cartilaginous and neural tissue can be seen (1-2, 118-123).

Cytopathology

Cytological smears show different cellular components that can be misdiagnosed as contamination or non-diagnostic. The preoperative diagnosis of primary malignant thyroid teratoma is difficult (1-2, 118-123). The cytological smears from a malignant teratoma reveal the high-grade nature of malignant cells such as nuclear pleomorphism and variable chromatin structure. Some cells may show powdery chromatin with indistinct nucleoli, suggestive of a neuroendocrine lineage. The presence of immature neuroepithelial small round blue cells is unlikely to be recognized on FNA (1-2, 118-122). The differential diagnosis includes high-grade malignant tumors with neuroendocrine differentiation such as MTC (positive for calcitonin and CEA) and small cell neuroendocrine carcinoma (keratin positive) (123-125). Neuroblastoma and Ewing sarcoma may also rarely involve the thyroid; such

tumors are essentially impossible to distinguish from malignant teratomas without histological samples.

Histopathology

In order to be defined as a thyroid teratoma, thyroid parenchyma should be identified within the mass (1-2, 118-125). Teratomas include a large variety of tissue types and growth patterns in a single lesion. The presence of cystic spaces and solid nests with different types of epithelium can be seen including squamous, glandular, cuboidal, pseudostratified ciliated columnar and transitional epithelium. The evidence of pilosebaceous and other skin adnexal tissues are documented (1-2). Neural tissue is commonly found and can be defined as mature and/or immature. Specifically, the maturation of neural-type tissue defines the grade, such as completely mature, predominantly mature, and exclusively immature (1-2, 118-125).

Ancillary studies

Immunohistochemistry can be used to confirm the various tissue types in a malignant teratoma (1-2). For example, S100 protein, glial fibrillary acidic protein, synaptophysin, and neurofilament protein are variably positive in neuroectodermal and glial components. MyoD1 and myogenin are useful to identify rhabdomyoblastic differentiation (1-2, 118-125).

Differential diagnosis

The differential diagnosis in a neonate includes lymphangioma, thyroglossal duct cyst and branchial cleft cyst. Other considerations in adult patients include MTC, Ewing sarcoma, rhabdomyosarcoma, small cell carcinoma, lymphoma and melanoma. The diagnosis relies on the identification of the various tissue types with the support of immunohistochemistry.

12. **CONCLUSION**

Non-epithelial thyroid tumors, both benign and malignant, represent an extremely rare group of lesions. Apart from their rarity in this location, given the morphologic overlap of these lesions with epithelial thyroid lesions and other similar appearing non-epithelial tumors that may involve the thyroid, reaching an accurate diagnosis based on cytology material alone is very challenging. Given the broad differential diagnosis for many of these conditions, the use of ancillary techniques such as immunohistochemistry and molecular testing is essential. Even though non-epithelial primary thyroid tumors are exceedingly rare, these entities should always be considered when evaluating a thyroid

FNA, especially when the cytomorphological features do not match the ultrasonographic, clinical or expected immunohistochemical findings.

REFERENCES

1) Thompson LDR. Rare primary thyroid nonepithelial tumors and tumor-like conditions. In Diagnostic Pathology and Molecular Genetics of the thyroid. Nikiforov YE, Biddinger PW, Thompson LDR 3rd Ed. Wolters Kluwer. 2020; 419-52

2) Wick MR, Eusebi V, Lamovec J et al. Tumors of the thyroid gland. In: Lloyd RV, Osamura RY, Kloppel G et al. eds World Health Organization Classification of tumors of endocrine organs. Lyon, France, IARC 2017

3) Surov A, Gottschling S, Wienke A et al. Primary thyroid sarcoma: a systematic review. Anticancer Res 2015; 35: 5185-91

4) Baloch ZW, LiVolsi VA. Unusual Tumors of the Thyroid Gland Endocrinol Metab Clin North Am. 2008; 37: 297-310

5) Geller RL, Hookim K, Sullivan HC et al. Cytologic features of angiosarcoma: A review of 26 cases diagnosed on FNA. Cancer Cytopathol 2016; 124: 659-68

6) Ito YK, Nakashima T, Mori T. Pathomorphologic characteristics of 102 cases of thorotrast-related hepatocellular carcinoma, cholangiocarcinoma and hepatic angiosarcoma. Cancer 1988; 62: 1153-62

7) Falk S, Krishnan J, Meis JM. Primar angiosarcoma of the spleen. A clinciopathologic study of 40 cases. Am J Surg Pathol 1993; 17: 959-70

8) Randall MB, Geisinger KR. Angiosarcoma of the heart: Pericardial fluid cytology. Diagn Cytopathol 1990; 6: 58-62

9) Lin O, Gerhard R, Coelho Siqueira SA, De Castro IV. Cytological findings of epithelioid angiosarcoma of the thyroid. A case report. Acta Cytol 2002; 46: 767-71

10) Hasegawa T, Fujii Y, Seki K et al. Epithelioid angiosarcoma of the bone. Hum Pathol 1997; 28: 985-89

11) Kuhn E, Ragazzi M, Ciarrocchi A et al. Angiosarcoma and anaplastic carcinoma of the thyroid are two distinct entities: a morphologic, immunohistochemical, and genetic study. Mod Pathol 2019; 32: 787-98

12) Boucher LD, Swanson PE, Stanley MW et al. Cytology of angiosarcoma. Findings in fourteen fine-needle aspiration biopsy specimen and one pleural fluid specimen. Am J Clin Pathol 2000; 114: 210-19

13) Liu K, Layfield LJ. Cytomorphologic features of angiosarcoma on fine needle aspiration biopsy. Acta Cytol 1999; 43: 407-15

14) Minimo C, Zakowski M, Lin O. Cytologic findings of malignant vascular neoplasms: A study of twenty-four cases. Diagn Cytopathol 2002; 26: 349-55

15) Miao J, Chen S, Li Y, Fu L, Lia H. Primary Cavernous Hemangioma of the Thyroid Gland: A Case Report and Literature Review Medicine (Baltimore). 2017; 96: e8651

16) Rice C.O. Hemangioendothelioma of thyroid gland. Amer. J. Cancer 1931; 15: 2301-2308

17) Chen KT, Kinkegaard DD, Bocian JJ. Angiosarcoma of the breast. Cancer 1980; 46: 368-71

18) Wick MR, Eusebi V, Lamovec J, Ryska A. Angiosarcoma In: Lloyd RV, Osamura RY, Klöppel G, Rosai J. WHO Classification of tumors of endocrine organs 4th Edition, Volume 10. IARC, Lione: 129-132

19) Vanderbussche CJ, Wakely PE, Siddiqui MT, Maleki Z, Ali SZ. Cytopathologic characteristics of epithelioid vascular malignancies. Acta cytol 2014; 58: 356-66

20) Thompson LD, Wenig BM, Adair CF, Heffess CS. Peripehral nerve sheath tumors of the thyroid gland. A series of four cases and a review of the literature. Endocr Pathol 1996; 7: 309-318

21) Nagavalli S, Yehuda M, McPhaul LW et al. A cervical schwannoma masquerading as a thyroid nodule. Eur Thyroid J 2017; 6: 216-20

22) Chen G, Liu Z, Su C et al. Primary peripheral nerve sheath tumors of the thyroid gland: A case report and literature review. Mol Clin Oncol 2016; 4: 209-10

23) Capelli A, Guernelli L, Bertoni F, Fuga G. Neurofibroma of the thyroid gland (report of a case). Arch Chir Torac Cardiovasc 1975; 32: 23-27

24) Gaud U, Shukla K, Kumar M, Pandey M. Isolated intrathyroidal neurofibroma. Otolaryngol Head Neck Surg 2009; 141: 300-1

25) Kandil E, Khalek MB, Abdullah O et al. Primary peripheral nerve sheath tumors of the thyroid gland. Thyroid 2010; 20: 583-86

26) Jayaram G. Neurilemmoma (schwannoma) of the thyroid diagnosed by fine needle aspiration cytology. Acta Cytol 1999; 43: 743-44

27) Baglaj M, Markowska-Woyciechowska A, Sawicz-Birkowska K et al. Primary neurilemmoma of the thyroid gland in a 12-year-old girl. J Pediatr SUrg 2004; 38: 1418-20

28) Yu GH, Sack MJ, Baloch Z, et al. Difficulties in the fine needle aspiration (FNA) diagnosis of schwannoma. Cytopathology 1999; 10: 186–94.

29) Zheng X, Guo K, Wang H, et al. Extracranial schwannoma in the carotid space: a retrospective review of 91 cases. Head Neck 2017; 39:42–7.

30) Kasraeian S, Allison DC, Ahlmann ER, et al. A comparison of fine-needle aspiration, core biopsy, and surgical biopsy in the diagnosis of extremity soft tissue masses. Clin Orthop Relat Res 2010; 468: 2992–3002.

31) Ahn D, Lee GJ, Sohn JH, et al. Fine-needle aspiration cytology versus core-needle biopsy for the diagnosis of extracranial head and neck schwannoma. Head Neck 2018; 40: 2695–700.

32) Kang JY, Yi KS, Cha SH et al. Schwannoma of the thyroid bed. A case report and review of literature. Medicine (Baltimore). 2020; 99: e18814

33) Wakely PE, Ali SZ, Bishop J. The cytopathology of malignant peripheral nerve sheath tumor. A report of 55 fine-needle aspiration cases. Cancer Cytopathol 2012; 120: 334-41

34) Miller DL, Thompson LDR, Bishop JA, Rooper LM, Ali SZ. Malignant teratomas of the thyroid gland: clinico-radiologic and cytomorphologic features of a rare entity. J Am Soc Cytopathol. 2020; 9: 221-231.

35) Schaefer IM, Fletcher C, Hornick JL. Loss of H3K27 trimethylation distinguishes malignant peripheral nerve sheath tumors from histologic mimics. Mod Pathol 2016; 29(1):4-13

36) Mito JK, Qian X, Doyle LA, Hornick JL, Jo V. Role of Histone H3K27 Trimethylation Loss as a Marker for Malignant Peripheral Nerve Sheath Tumor in Fine-Needle Aspiration and Small Biopsy SpecimensAm J Clin Pathol 2017; 148: 179-89

37) Cetin S, Kir G, Yilmaz M. Thyroid paraganglioma diagnosed by fine needle aspiration biopsy, correlated with histopathological findings. Report of a case. Diagn Cytopathol 2016; 44: 643-47

38) Kiriakopoulos A, Linos D. Thyroid paraganglioma: A case report of a rare head and neck tumor. J Surg Case Rep 2018; 8: 1-3

39) Lack EE, Cubila AL, Woodruff JM. Paragangliomas of the head and neck region. A pathologic study of tumors from 71 parents. Hum Pathol 1979; 10: 191-218

40) Baloch ZW, LiVolsi VA. Neuroendocrine tumors of the thyroid gland. Am J Clin pathol 2002; 115: 556-67

41) De Tullio A, Lisco G, Duda l, Renzulli G, Triggiani V. Medullary thyroid cancer with paraganglioma-like pattern diagnosed during pregnancy: A case report and literature revision. Endocr Metab Immune Disord Drug Targets. 2020; 20: 295-302

42) Zhang W, Policarpio-Nicolas MLC. Aspiration cytology of primary thyroid paraganglioma. Diagn Cytopathol 2015; 43: 838-43

43) LaGuette J, Matias-Guiu X, Rosai J. Thyroid paraganglioma: A clinicopathologic and immunohistochemical study of three cases. Am J Surg Pathol 1997; 21: 748-52

44) Plaza JA, Wakely PE Jr, Moran C, Fletcher CD, Suster S Sclerosing paraganglioma: report of 19 cases of an unusual variant of neuroendocrine tumor that may be mistaken for an aggressive malignant neoplasm Am J Surg Pathol. 2006; 30(1):7-11

45) Von Dobschuetz E, Leijon H, Schalin-Jantti C et al. A registry-based study of thyroid paraganglioma: histological and genetics characteristics. Endocr Relat Cancer 2015; 22: 191-204 .

46) Johnson TL, Zarbo RJ, Lloyd RV, Crissman JD. Paragangliomas of the head and neck: immunohistochemical neuroendocrine and intermediate filament typing. Mod Pathol. 1988; 1(3):216-23.

47) Satturwar S, Rossi ED, Maleki Z, Canton R, Faquin W, Pantanowitz L. Thyroid paraganglioma: A diagnostic pitfall in thyroid FNA. *Cancer Cytopathology* In press.

48) Costinean S, Balatti V, Bottoni A et al. Primary intrathyroidal paraganglioma: histopathology and novel molecular alterations. Human Pathol 2012; 43: 2371-75

49) Zantour B, Guilhaume B, Tissier F et al. A thyroid nodule revealing a paraganglioma in a patient with a new germline mutation in the succinate dehydrogenase B gene. Eur J Endocrinol 2004; 151; 433-38

50) Kaushal S, Iyer VK, Mathur SR, Ray R. Fine needle aspiration cytology of medullary carcinoma of the thyroid with a focus on rare variants: A review of 78 cases. Cytopathol 2011; 22; 95-106

51) Milias S, Hytiroglou P, Kourtis D et al. Granular cell tumor of the thyroid gland. Histopathology 2004; 44: 190-91

52) Abrikossoff A. Uber myome ausgehend von der quergestreiften willkurlichen muskulatur. Virchows Arch Pathol Anat 1926; 260: 215-233

53) Finer EB, Villalba JA, Pitman MB et al. Granular cell tumor of the lung. Diagn Cytopathol. 2019; 47: 345-346.

54) Corso G, Di Nubila B, Ciccia A et al.Granular cell tumor of the breast: Molecular pathology and clinical management. Breast J. 2018; 24: 778-782

55) Ulivieri S, Muscas G, Lavalle L et al. Granular cell tumor of the orbit: pathological features and treatment. J Neurosurg Sci. 2017; 61: 342-343

56) Domínguez-González M, Nogales-Pérez A, Vázquez Navarrete S, et al. Granular cell tumor of the vulva. J Low Genit Tract Dis. 2013; 17: 82-4.

57) Almaghrabi M, Almaghrabi H, Al-Magrhabi H. Granular Cell Tumor of Thyroid: Challenging Pitfalls and Mimickers in Diagnosis. J Microsc Ultrastruct. 2020; 8: 1–6.

58) Bowry M, Almeida B, Jeannon JP. Granular cell tumour of the thyroid gland: A case report and review of the literature. Endocr Pathol. 2011; 22: 1–5.

59) Xu D, Zhuang S, Liao S, Lv Y, Yu J. Granular cell tumor of the thyroid in a 16-year-old girl: A rare entity. Int J Clin Exp Pathol. 2016; 9: 1499–503.

60) Du ZH, Qiu HY, Wei T, Zhu JQ. Granular cell tumor of the thyroid: Clinical and pathological characteristics of a rare case in a 14-year-old girl. Oncol Lett. 2015; 9: 777–9.

61) Park WC, Choi SH, Lee YS. Granular cell tumor of the thyroid gland: A case report and review of the literature. Korean J Endocr Surg. 2015; 15: 20–4.

62) Chen Q, Li Q, Guo L, Li S, Jiang Y. Fine needle aspiration cytology of a granular cell tumor arising in the thyroid gland: A case report and review of literature. Int J Clin Exp Pathol. 2014; 7: 5186–91.

63) Harp E, Caraway NP. FNA of thyroid granular cell tumor. Diagn Cytopathol. 2013; 41: 825–8.

64) Min KW, Paik SS, Jun YJ, Han H, Jang KS. Fine needle aspiration cytology of a granular cell tumour arising in the thyroid gland. Cytopathology. 2012; 23: 411–2.

65) Singh S, Gupta N, Sharma S, Azad RK. Aspiration cytology in the preoperative diagnosis of granular cell tumor of thyroid region in an 11-years-old female child. J Cytol. 2013; 30: 218–9.

66) Klemperer P, Rabin CB. Primary neoplasms of the pleura: a report of five cases. Arch Pathol 1931; 11: 385-412

67) Papi G, Corradi S, LiVolsi VA. Primary spindle cell lesions of the thyroid gland. An overview. Am J Clin Pathol 2005; 124: S95-S123

68) Deng XR, Wang G, Kuang CJ et al. Metastasis of leiomyosarcoma of the thyroid. Cin Med J 2005; 118: 174-76

69) Sahin MI, Vurl A, Yuce I et al. Thyroid leiomyosarcoma: presentation of two cases and review of the literature. Braz J Otorhinolaryngol 2016; 82: 715-21

70) Canu GL, Bulla JS, Lai ML et al. Primary thyroid leiomyosarcoma: A case report and review of the literature. G Chir 2018; 39: 51-56

71) D'andrea N, Romano V, Mattioli F et al. Pulmonary artery leiomyosarcoma with thyroid metastases. Monaldi Arch Chest Dis 2003; 59: 304-307

72) Biankin SA, Cachia AR. Leiomyoma of the thyroid gland. Pathology 1999; 31: 48-66

73) Thompson LD, Wenig BM, Adair CF et al. Primary smooth muscle tumors of the thyroid gland. Cancer 1997; 79: 579-87

74) Ozaki O, Sugino K, Mimura T et al. Primary leiomyosarcoma of the thyroid gland. Surg Today 1997; 27: 177-80

75) Chetty R, Clark SP, Dowlin JP. Leiomyosarcoma of the thyroid: immunohistochemical and ultrastructural study. Pathology 1993; 25: 203-205

76) Black M, Wei XJ, Sun W et al. Adult rhabdomyoma presenting as thyroid nodule on fine needle aspiration in patient with BIRT-Hogg-Dube' syndrome: Case report and literature review. Diagn Cytopathol 2020; 48: 576-80

77) Purgina B, Rao UNM, Miettinen M, Pantanowitz L. AIDS-related EBV-associated smooth muscle tumors: A review of 64 published cases. Path Res Int 2011; 10: 561548.

78) Taccagni G, Sambade C, Nesland J, Terreni MR, Sobrinho-Simoes M. Solitary fibrous tumor of the thyroid: Clinico-pathological, immunohistochemical and ultrastructural study of three cases. Virchows Arch A Pathol Anat Histopathol 1993; 422: 491-97

79) Mizuuchi Y, Yamamoto H, Nakamura K et al. Solitary fibrous tumor of the thyroid gland. Med Mol Morphol 2014; 47: 117-22

80) Parwani AV, Galindo R, Steinberg D et al. Solitary fibrous tumor of the thyroid: Cytopathologic findings and differential diagnosis. Diagn Cytopathol 2003; 28: 213-16

81) Doyle LA, Vivero M, Fletcher CD, Mertens F, Hornick JL. Nuclear Expression of STAT6 Distinguishes Solitary Fibrous Tumor From Histologic Mimics. Mod Pathol 2014; 27: 390-95

82) Demicco EG, Wagner MJ, Maki RG et al. Risk assessment in solitary fibrous tumors: validation and refinement of a risk stratification model. Mod Pathol 2017; 30: 1433-42

83) Westra WH, Gerald WL, Rosai J. Solitary fibrous tumor. Consistent CD34 immunoreactivity and occurrence in the orbit. Am J Surg Pathol 1994; 18: 992-98

84) Suster D, Michal M, Nishino M et al. Papillary thyroid carcinoma with prominent myofibroblastic stromal component: clinicopathologic, immunohistochemical and next-generation sequencing study of seven cases. Mod Pathol 2020; 33: 1702-11

85) Yu l, Yang SJ. Primary Follicular dendritic cell Sarcoma of the thyroid gland coexisting with hashimoto thyroiditis. Int J Surg Pathol 2011; 19: 502-505

86) Fonseca R, Yamakawa M, Nagkamura S et al. Follicular dendritic cell sarcoma and interdigitating reticulum cell sarcoma: A review. Am J Hematol 1998; 59: 161-67

87) Monda L, Warnke R, Rosai J. A primary lymph node malignancy with features suggestive of dendritic reticulum cell differentiation. A report of 4 cases. Am J Pathol 1986; 122: 562-72

88) Jabbour MN, Fedda FA, Tawil AN, Shabb NS, Boulos FI. Follicular dendritic cell sarcoma of the head and neck expressing thyroid transcription factor-1: a case report with clinocopathologic and immunohistochemical literature review. Appl Immunohistochem Mol Morphol 2014; 22: 705-12

89) Davila J, Starr JS, Attia S et al. Comprehensive genomic profiling of a rare thyroid follicular dendritic cell sarcoma. Rare Tumors 2017; 9: 6834-37

90) Starr JS, Attia S, Joseph RW et al. Follicular dendritic cell sarcoma presenting as a thyroid mass. J Clin Oncol 2015; 33: e74-76

91) Galati LT, Barnes EL, Myers EN. Dendritic cell sarcoma of the thyroid. Head and Neck 1999; 21: 273-75

92) Layfield LJ, Kakudo K. Metastatic tumors, lymphoma and rare tumors of the thyroid. Ali S, Cibas ES. The Bethesda system for reporting thyroid cytopathology. 2nd Edition, Springer, Berlin. 2018; 218-221

93) Griffin GK, Sholl LM, Lindeman NI, Fletcher CD, Hornick JL. Targeted genomic sequencing of follicular dendritic cell sarcoma reveals recurrent alterations in NF-κB regulatory genes Mod Pathol. 2016; 29: 67-74.

94) Pusztaszeri M, Sauder K, Cibas ES, Faquin WC. Fine-needle aspiration of primary Langerhans cell histiocytosis of the thyroid gland, a potential mimic of papillary thyroid carcinoma. Acta Cytol 2013; 57: 406-12

95) Harmon CM, Brown N. Langerhans Cell Histiocytosis: A Clinicopathologic Review and Molecular Pathogenetic Update. Arch Pathol Lab Med. 2015; 139: 1211-4.

96) Pandyaraj RA, Sathik M, Masoodu K, Maniselvi S, Savitha S, Divya D, Pandyaraj RA, et al. Langerhans cell histiocytosis of thyroid-a diagnostic dilemma. Indian J Surg. 2015; 77: 49-51

97) Saqi A, Kuker AP, Ebner SA, et al. Langerhans Cell Histiocytosis: Diagnosis on Thyroid Aspirate and Review of the Literature. Head Neck Pathol. 2015; 9: 496-502

98) Ceyran AB, Senol S, Bayraktar B et al. Langerhans cell histiocytosis of the thyroid with multiple cervical lymph node involvement accompanying metastatic thyroid papillary carcinoma. Case Rep Pathol. 2014: 184237.

99) Xia CX, Li R, Wang ZH, et al A rare cause of goiter: Langerhans cell histiocytosis of the thyroid. Endocr J. 2012; 59 :47-54.

100) Gul OO, Sisman P, Cander S et al. An unusual case of adult-onset multi-systemic Langerhans cell histiocytosis with perianal and incident thyroid involvement. Endocrinol Diabetes Metab Case Rep. 2017 2:16-0087

101) Behrens RJ, Levi AW, Westra WH, Dutta D, Cooper DS, Behrens RJ, et al. Langerhans cell histiocytosis of the thyroid: a report of two cases and review of the literature. Thyroid. 2001; 11: 697-705.

102) Patten DK, Wani Z, Tolley N, Patten DK, et al. Solitary Langerhans histiocytosis of the thyroid gland: a case report and literature review. Head Neck Pathol. 2012; 6: 279-89

103) Wu X, Chen S, Zhang LY et al. Langerhans cell histiocytosis of the thyroid complicated by papillary thyroid carcinoma. A case report and brief literature review. Medicine (Baltimore) 2017; 96: e7954

104) Guarino S, Giusti DM, Rubini A et al. Association between pituitary Langerhans cell histiocytosis and papillary thyroid carcinoma. Clin Med Insights Case Rep 2013; 9: 197-200

105) Moschovi M, Adamaki M, Vlahopoulos S, Rodriguez-Galindo C. Synchronous and metachronous thyroid cancer in relation to Langerhans cell histiocytosis; involvement of V600E BRAF-mutation? Pediatr Blood Cancer. 2015; 62: 173-4

106) Phulware RH, Guleria P Iyer VK et al. Cytological diagnosis of Langerhans cell histiocytosis: A series of 47 cases. Cytopathol 2019; 30: 413-418.

107) Hang JF, Siddiqui MT, Ali SZ. Fine Needle Aspiration of Langerhans Cell Histiocytosis: A Cytopathologic Study of 37 Cases. Acta Cytol. 2017; 61: 96-102

108) Al Hamad M, Albisher HM, Al Saeed WR et al. BRAF gene mutations in synchronous papillary thyroid carcinoma and Langerhans cell histiocytosis co-existing in the thyroid gland: a case report and literature review. BMC Cancer. 2019; 19: 170.

109) Kuhn E, Ragazzi M, Zini M et al. Critical Pitfalls in the use of BRAF Mutation as a Diagnostic Tool in Thyroid Nodules: a Case Report. Endocr Pathol. 2016; 27: 220-3

110) Vujhini SK, Kolte SS, Satarkar RN, Srikanth S. Fine Needle Aspiration Diagnosis of Rosai-Dorfman Disease Involving Thyroid. J Cytol. 2012; 29: 83-85.

111) Giannella P, Dulguerov N, Arnoux G, Pusztaszeri M, Seebach JD. Thyroid Rosai-Dorfman disease with infiltration of IgG4-bearing plasma cells associated with multiple small pulmonary cysts. BMC Pulmonary Medicine 2019; 19: 83-87

112) Emile JF, Abla O, Fraitag S et al. Histiocyte society. Revised Classification of histiocytoses and neoplasms of the machropage-dendritic cell lineage. Blood 2016; 127: 2672-81

113) Rosai J, Dorfman RF. Sinus histiocytosis with massive lymphadenopathy. A newly recognized benign clinicopathological entity. Arch Pathol 1969; 87: 63-70

114) Foucar E, Rosai J, Dorfman RF. Sinus histiocytosis with massive lymphadenopathy (Rosai-Dorfman disease): Review of the entity. Semin Diagn Pathol 1990; 7: 19-73

115) Lee FY, Jan YJ, Chou G, Wang J, Wang CC. Thyroid involvement in Rosai-Dorfman disease. Thyroid 2007; 17: 471-6

116) Palmas Candia F, Porras Ledantes JA, Raventós Estellé A, Simón Muela I, Vendrell Ortega J, Näf Cortés S. Thyroid Involvement by Rosai-Dorfman Disease Endocrinol Diabetes Nutr. 2017; 64: 280-281

117) Powell GJ, Goellner JR, Nowak LE, McIver B. Rosai-Dorfman Disease of the Thyroid Masquerading as Anaplastic Carcinoma. Thyroid 2003; 13: 217-21

118) Oak CY, Kim HK, Yoon TM et al. Benign teratoma of the thyroid gland. Endocrinol Metab 2013; 28: 144-48

119) Riedlinger WF, Lack EE, Robson CD, rAHbar R, Nose' V. Primary thyroid teratomas in children: a report of 11 cases with a proposal of criteria for their diagnosis. Am J Surg Pathol 2005; 29: 700-6

120) Thompson LDR, Rosai J, Heffess CS. Primary thyroid teratomas: A clinicopathologic study of 30 cases. Cancer 2000; 88: 1149-58

121) Jayaram G, Cheah PL, Yip CH. Malignant teratoma of the thyroid with predominantly neuroepithelial differentattion: fine needle aspiration cytologic, histologic and immunocytochemical features of a case. Acta Cytol 2000; 44: 375-9

122) Martins T, Carriho F, Gomes L et al. Malignant teratoma of the thyroid gland: Case report. Thyroid 2006; 16: 1311-13

123) Starling CE, Sabra J, Brady B, Horton M, Traweek ST. Malignant teratoma of the thyroid. A difficult diagnosis by fine-needle aspiration. Diagn Cytopathol 2019; 47: 930-34

124) Cibas ES, Ali SZ. Medullary thryoid carcinoma. The 2017 Bethesda system for reporting thyroid cytopathology. Springer international; 2017: 157-75

125) Can AS, Koksal G. Thyroid metastasis from small cell lung carcinoma: A case report and review of the literature. J Med Case reports. 2015; 9: 231.

Table 1. Cytomorphologic overlap between non-epithelial and epithelial lesions of the thyroid gland.

Cytomorphology	Non-epithelial thyroid disease	Epithelial thyroid disease
Nuclear grooves	LCH	PTC, HTT, some MTC
Nuclear pseudoinclusions	LCH	HTT, PTC, some MTC
Spindle nuclear features	FDCT, GCT, leiomyoma, leiomyosarcoma, PNST, MPNST, paraganglioma, SFT	HTT, some PTC, MTC, metastases including melanoma
Voluminous cytoplasm	FDCT, GCT, LCH, paraganglioma, RDD	Oxyphilic neoplasms including oxyphilic variant of PTC and/or MTC, metastases
Granular cytoplasm	Angiosarcoma, GCT, LCH, paraganglioma, RDD	Oxyphilic neoplasms including oxyphilic variant of PTC and/or MTC, metastases
Naked nuclei	GCT, paraganglioma	HTT, MTC, PTC, metastases

FDCT: Follicular dendritic cell tumor; GCT: Granular cell tumor; HTT: Hyalinizing trabecular tumor; LCH: Langerhans cell histiocytosis; MTC: Medullary thyroid carcinoma; MPNST: Malignant peripheral nerve sheath tumor; PNST: Peripheral nerve sheath tumor, PTC: Papillary thyroid carcinoma; RDD: Rosai-Dorfman disease; SFT: Solitary fibrous tumor

Table 2 Cytologic features of non-epithelial spindle cell tumors of the thyroid

	Leiomyoma	**Leiomyosarcoma**	**PNST**	**MPNST**	**SFT**	**Settle**
Clinical findings	Thyroid mass Variable size	Thyroid mass Mean size 6cm Infiltrative pattern	Gradually enlarging mass	Mass increasing in size Infiltrative pattern	Well-defined mass Mean size 4.5cm	Long-standing mass Circumscribed to infiltrative
ultrasound features	Hypoechoic, cold nodule	Ill-defined hypoechoic mass with halo	Circumscribed hypoechoic mass	Infiltrative hypoechoic mass	Solid or hyperechoic nodule	Solid or cystic hypoechoic mass
morphological architecture	Cluster of spindle-shaped monomorphic cells	Clusters of atypical spindle cells	Clusters of spindle cells	Clusters of highly atypical spindled/epithelioid cells in a loosely hemorrhagic and/or necrotic background	Dyscohesive clusters of cells intermingled with amorphous pink stromal tissue Naked nuclei	highly cellular, lobular cohesive clusters, isolated cells, metachromatic extracellular material in granules or clumps
cytoplasm	Scant	Scant	scant	Fibrillary cytoplasm	scant	Scant fibrillar
nuclei	Monomorphic spindled	Pleomorphic and atypical spindled	Slender wavy and spindled	Atypical, pleomorphic fusiform Typical and atypical mitotic figures	spindle	Bland uniform spindle
nucleoli	Inconspicuous	Inconspicuous	Inconspicuous	inconspicuous	inconspicuous	Inconspicuous
ICC positivity	Desmin, SMA, H-caldesmon, muscle-specific actin	Desmin, SMA, H-caldesmon, muscle-specific actin	S100, SOX10	S100, SOX10, loss of H3K27me3	STAT6, CD34	Keratins

LEGEND: ATC: Anaplastic thyroid carcinoma; HTT: Hyalinizing trabecular tumor; LCH: Langerhans cell histiocytosis; MPNST: Malignant peripheral nerve sheath tumor; PNST: Peripheral nerve sheath tumors; SFT: Solitary fibrous tumor; SMA: Smooth muscle actin

Table 3. Table comparing the cytopathology of granular thyroid gland lesions

Diagnosis	**Granular Cell Tumor**	**Hürthle cell neoplasm/lesion**	**Medullary thyroid carcinoma**
Cell arrangement	Clusters & single cells	Clusters ± single cells	Clusters ± single cells
Cell borders	Indistinct	Distinct	Distinct
Cytoplasm	Fine granules	Fine granules	Red granules
Nucleus	Round with nucleoli	Round with nucleoli	Round without nucleoli
Background	Granular	Clean	Amyloid

Legends for the pictures

Figure 1. Hemangioma. Figure 1 shows cytological details of a hemangioma. The picture is characterized by single spindle-shaped cells with swirls of endothelial cells. (Diff-Quick, 8x)

Figures 2a-d. **Angiosarcoma.** Figures 2a-b show the cytological features of a thyroid angiosarcoma (Diff Quick 40x, Pap stain 40x). The slides are hypercellular and composed of cells showing spindle-epithelioid and plasmacytoid features. Moderate cytoplasm and large nuclei with moderate to severe atypia can be seen. Figure 2c shows morphologic details from a histological case of thyroid epithelioid angiosarcoma defined by nests and sheets of epithelioid cells with eosinophilic cytoplasm (H&E, 40x). Figure 2d demonstrates the expression of CD31 in neoplastic cells (A&B10x).

Figures 3a–b. **Schwannoma**. Cytological details from a case of schwannoma. The cytological pictures show spindle cells with elongated and wavy nuclei, embedded in a metachromatic stroma. (Diff-Quick 20x and 40x)

Figures 4a-d. **Malignant Peripheral Nerve Sheath Tumor.** Figures 4a-b show smears with syncytial cell clusters of uneven size and cellularity characterized by a 3-dimensional effect leading to the inability to observe cells in the center of these aggregates. The majority of cells are uniform in size and shape with oval and/or elongated nuclei with smooth contours and inconsistently tapered or blunt-ended (diff-Quick 40x and Pap stain 20x). Figure 4c shows details from a case of malignant peripheral nerve sheath tumor (MPNST) with increased cellularity with spindled cells with marked nuclear atypia arranged in highly cellular fascicles (H&E 40x). Figure 4d shows loss of histone H3K27me3 (histone H3 with lysine 27 trimethylation) by immunohistochemistry (A&B 40x).

Figures 5a-d. Paraganglioma. Figure 5a and 5b show details from a paraganglioma of the thyroid gland. The smears show single cells or loose clusters of cells, with epithelioid, plasmacytoid and spindle features. Nuclear overlapping and crush artifact may be seen (Diff-Quick 10x). Figure 5c-5d show details from the histological features of the same FNA case. The images show a solid pattern with intratumoral sclerosis. Neoplastic cells have small-medium sized nuclei with round-to-oval shape and small nucleoli. (H&E 40x).

Figures 6a-c. Granular Cell Tumor. Figures 6a and 6b show cytological details from a case of a granular cell tumor that involved the thyroid gland. The smears show a pattern defined by single cells or syncytial clusters of cells with indistinct cell borders, fragile cytoplasm and eosinophilic cytoplasmic granules. (Diff-Quick 20x; Pap stain 60x). Figure 6c shows histological features of a granular cell tumor obtained from a cell-block. Large cells with an epithelioid and polygonal appearance show granular eosinophilic cytoplasm. (H&E, 40x)

Figures 7. Leiomyosarcoma. Cytological smear from a leiomyosarcoma. This cytological smear shows a cluster of spindle–shaped cells with a disordered fascicular growth pattern and pleomorphic nuclei (Diff-Quick 40x).

Figures 8a-b. Solitary Fibrous Tumor. Figure 8a is of a solitary fibrous tumor (SFT). The figure shows a paucicellular smear with slender discohesive spindle-shaped cells intermingled with amorphous collagenized stromal tissue (Pap stain 60x). Figure 8b represents the histological features from a SFT. Note the patternless appearance of the spindle cells and characteristic branching vessels (H&E 20x)

Figures 9. Follicular Dendritic Cell Sarcoma. Figure 9 shows histology of an FDC sarcomas characterized by syncytial sheets of epithelioid cells with round-ovoid vesicular nuclei, with delicate nuclear membranes and prominent nucleoli. (H&E 40x)

Figures 10a-b. Langerhans Cell Histiocytosis. Figure 10a shows the FNA of a case of Langerhans cell histiocytosis with a mixture of mononuclear and multinucleated histiocytoid cells, some with foamy granular cytoplasm (Diff-Quick 20x). Figure 10b illustrates Langerin positive cells (A&B 40x).

Figures 11a-d. **Rosai-Dorfman Disease.** Figures 11a and b show large histiocytes with abundant cytoplasm, indistinct cell borders, emperipolesis, and round vesicular nuclei. Inflammatory cells, such as lymphocytes can be seen in the cytoplasm (Diff-Quick 40x). Figure 11c shows histologic features consisting of a variable mix of large histiocytes with voluminous cytoplasm as well as lymphocytes, plasma cells and neutrophils. (H&E 40X). Figure 11d shows positivity for S100 (A&B 40x)

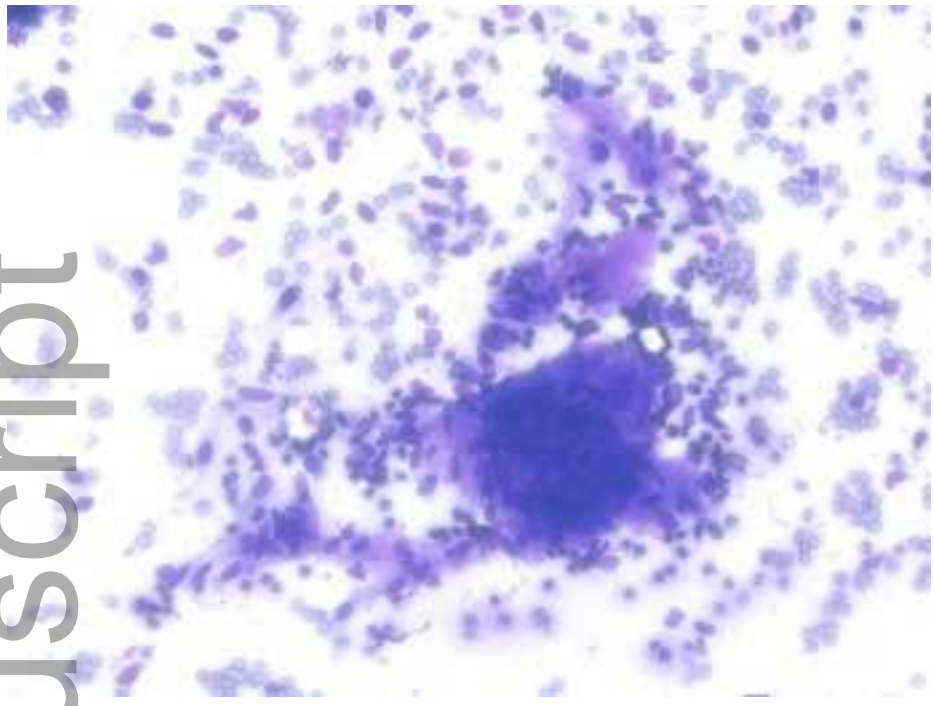

cncy_22404_f1.tif

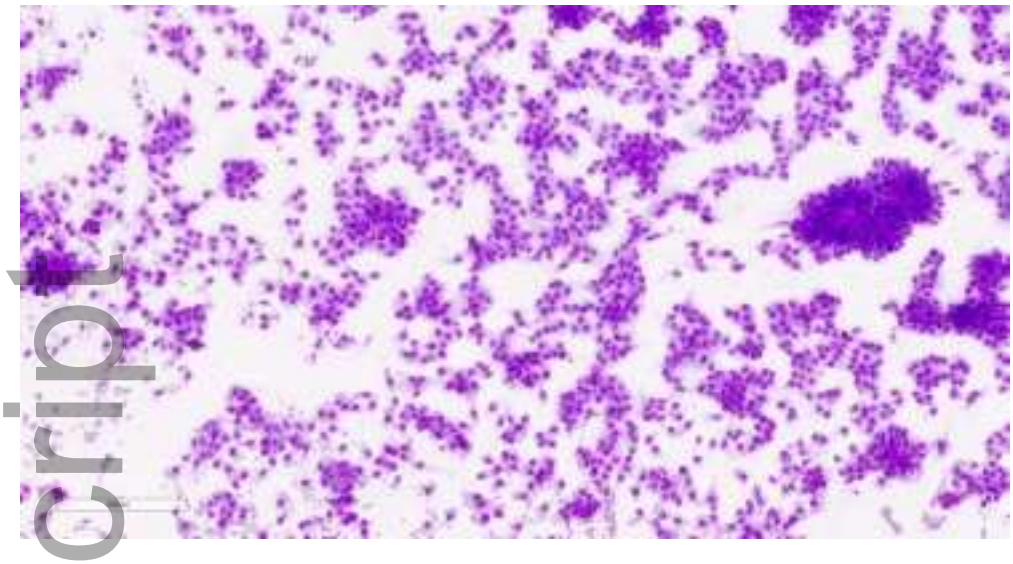

cncy_22404_f2a.tif

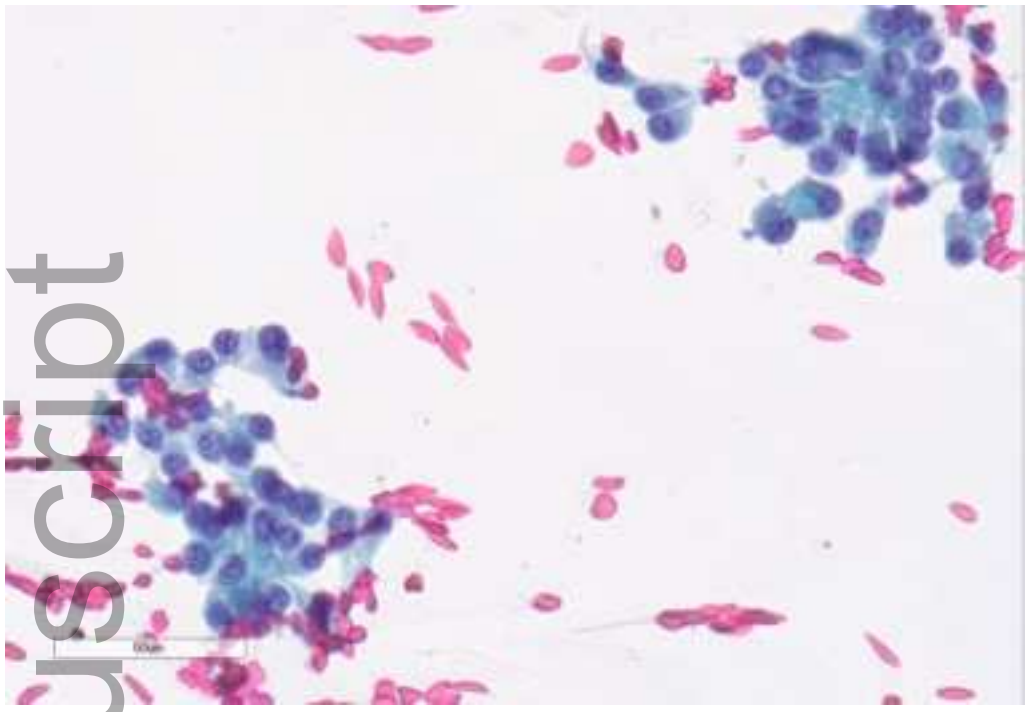

cncy_22404_f2b.tif

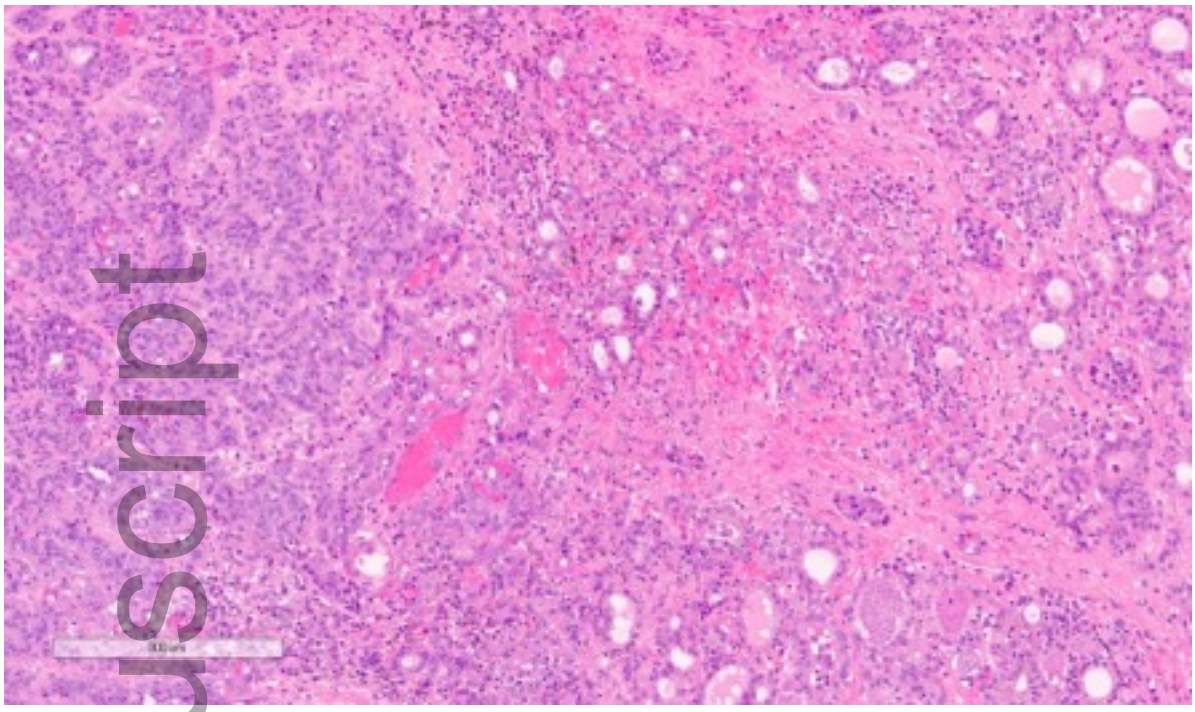

cncy_22404_f2c.tif

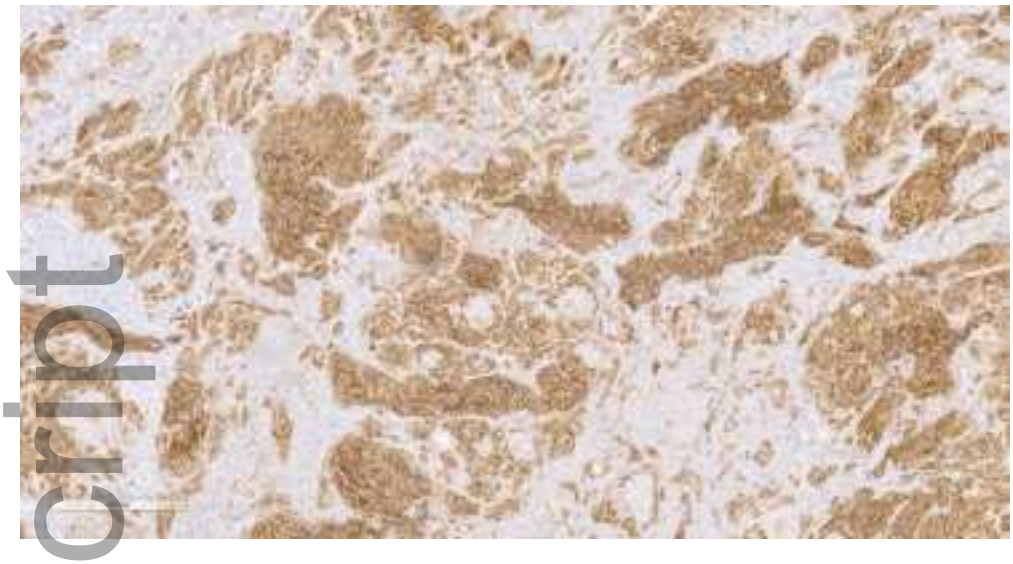

cncy_22404_f2d.tif

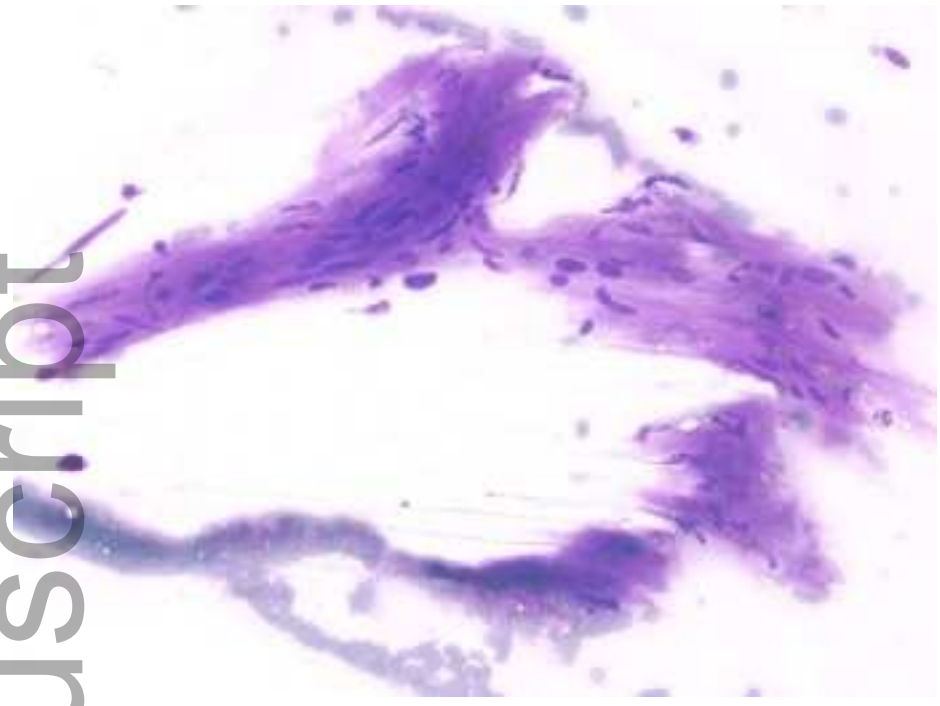

cncy_22404_f3a.tif

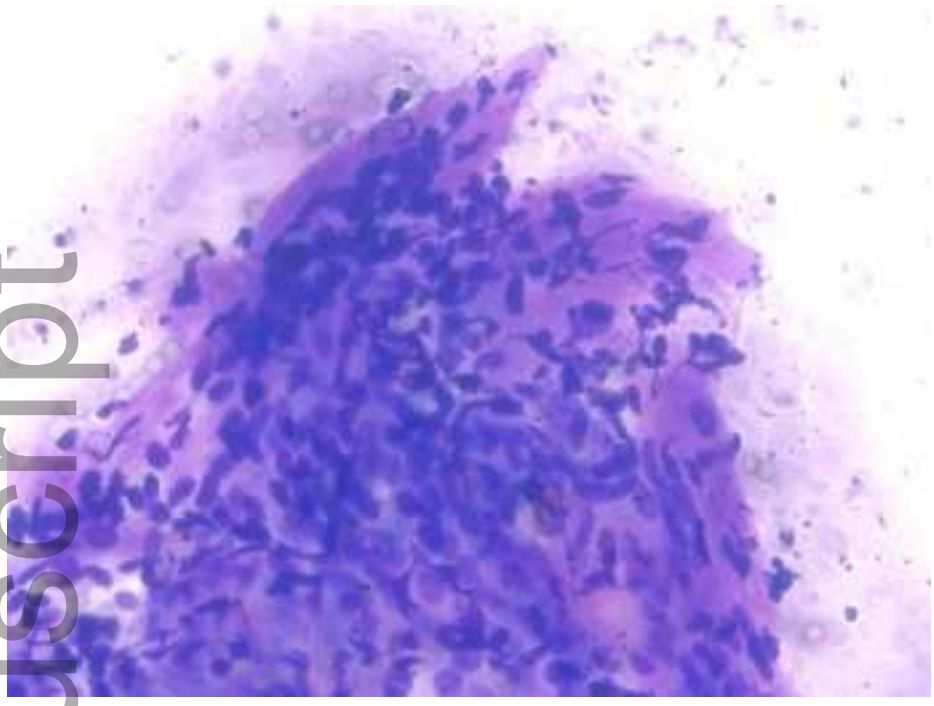

cncy_22404_f3b.tif

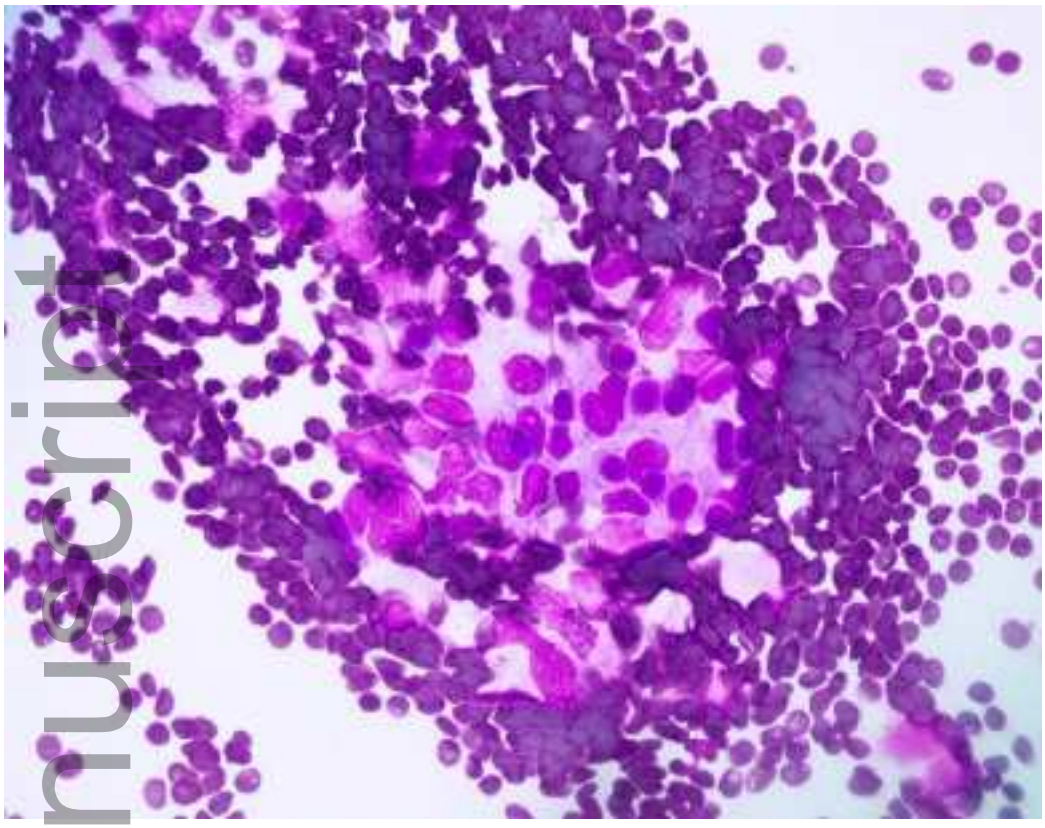

cncy_22404_f4a.tif

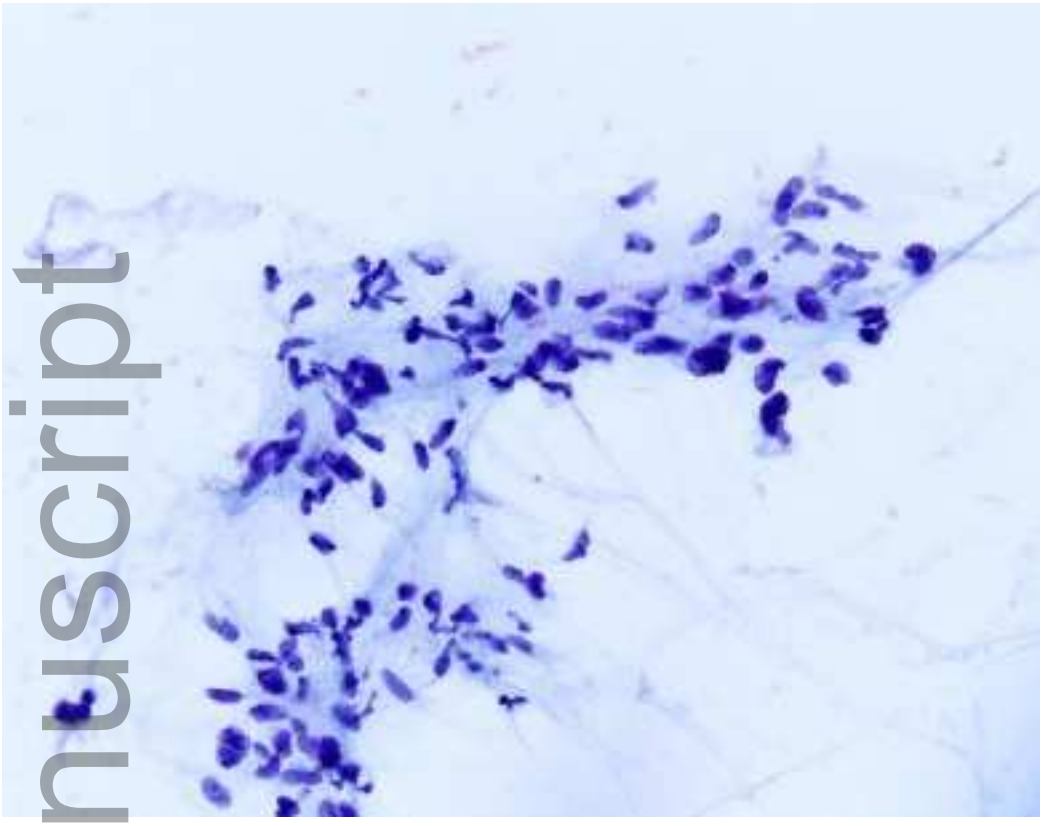

cncy_22404_f4b.tif

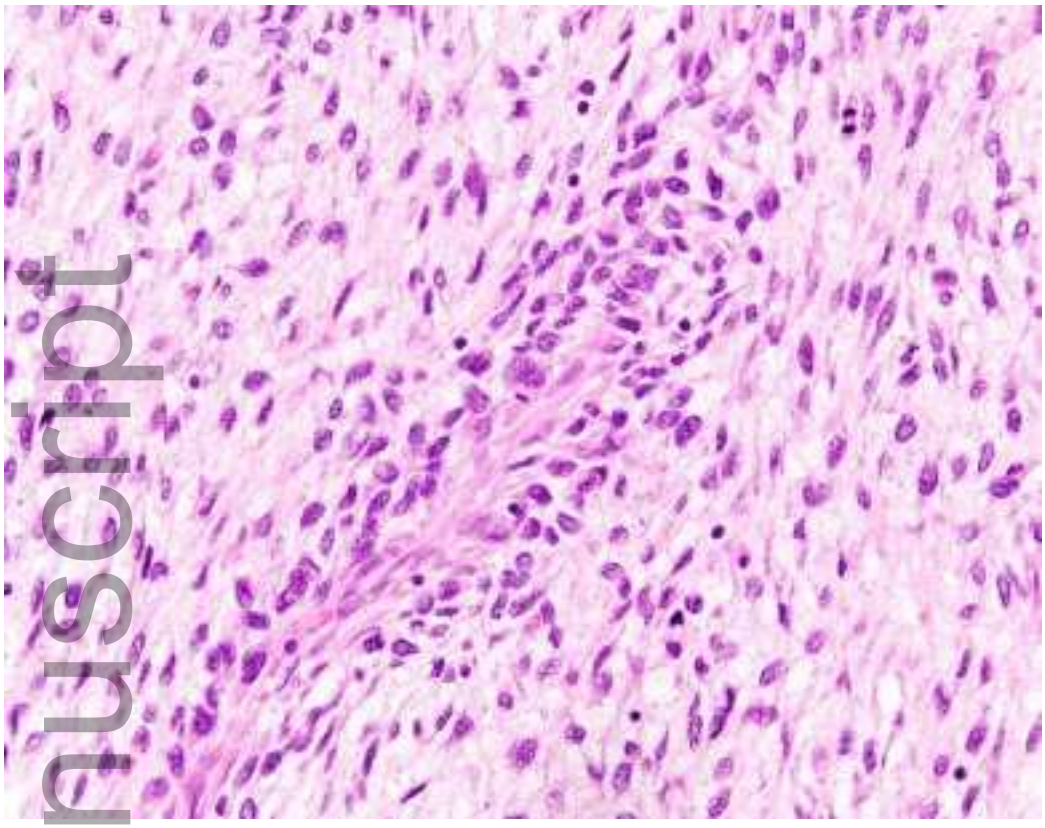

cncy_22404_f4c.tif

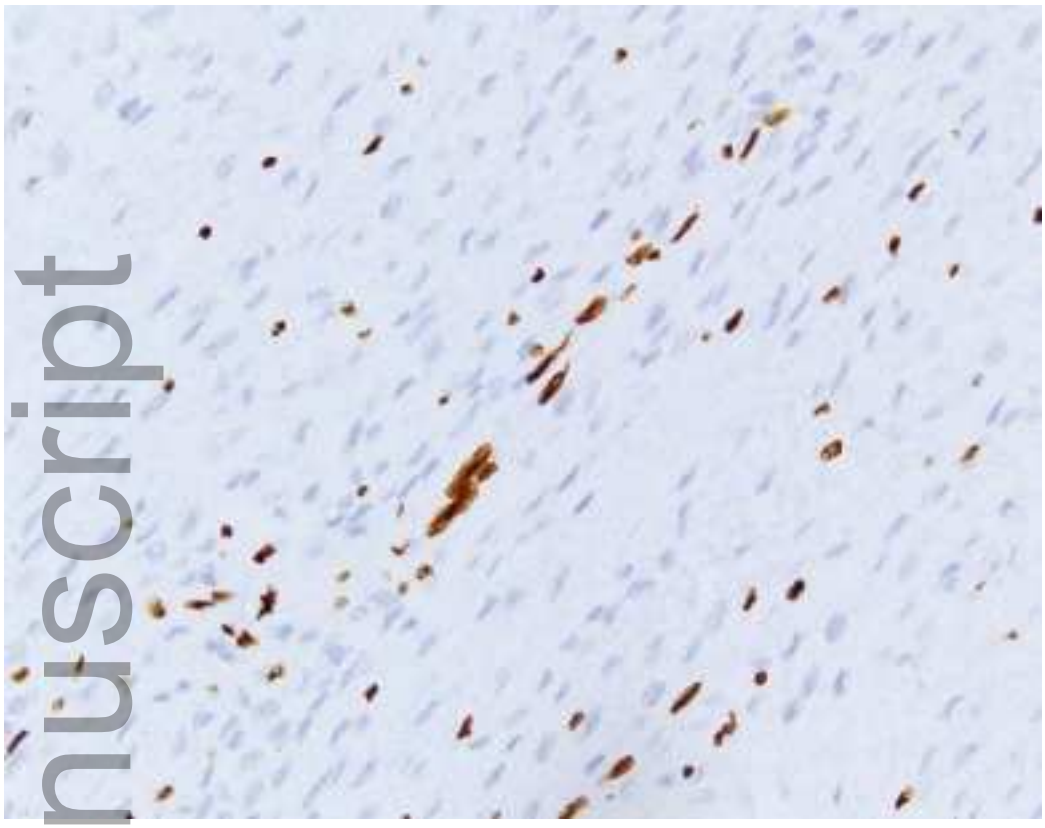

cncy_22404_f4d.tif

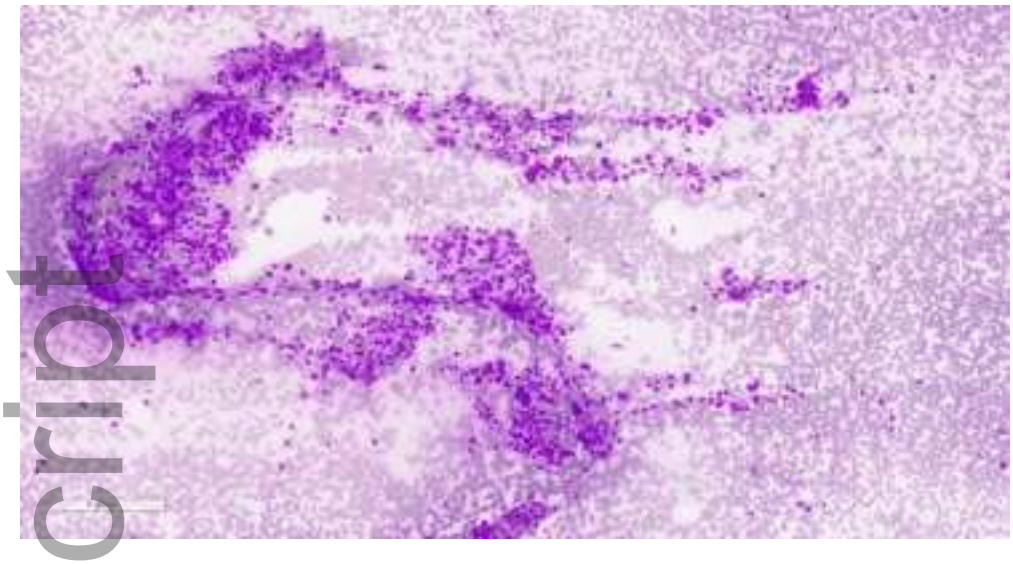

cncy_22404_f5a.tif

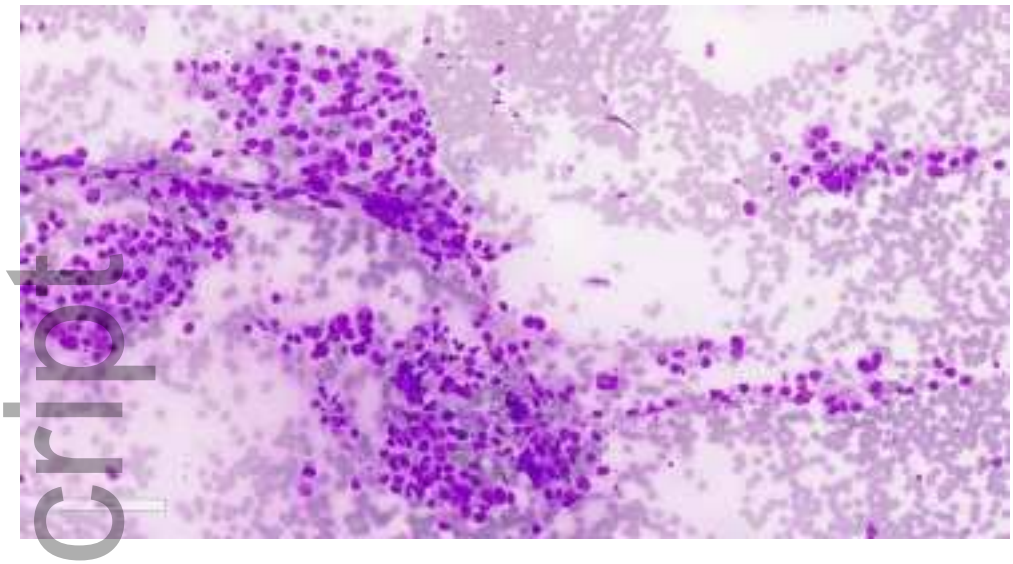

cncy_22404_f5b.tif

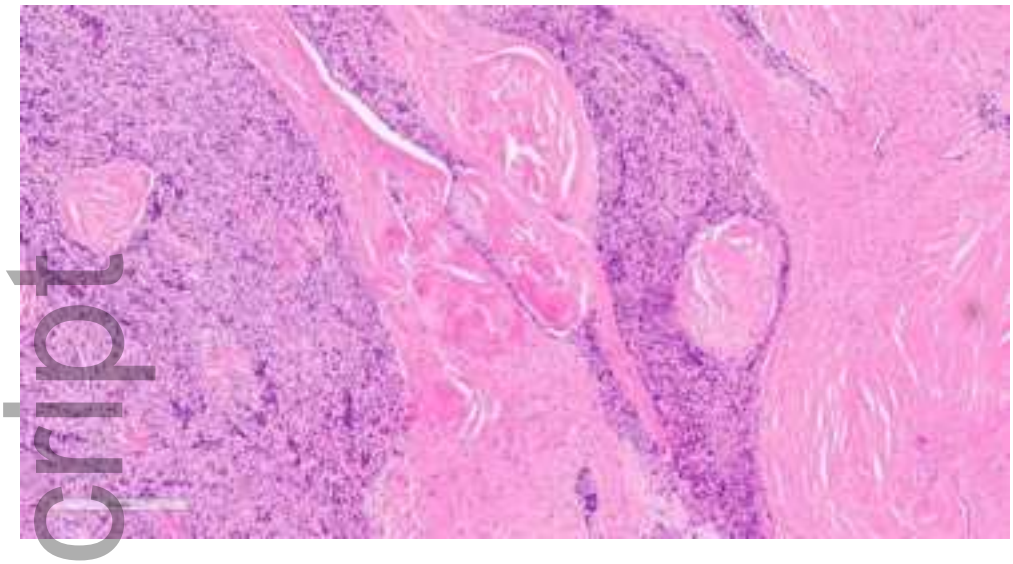

cncy_22404_f5c.tif

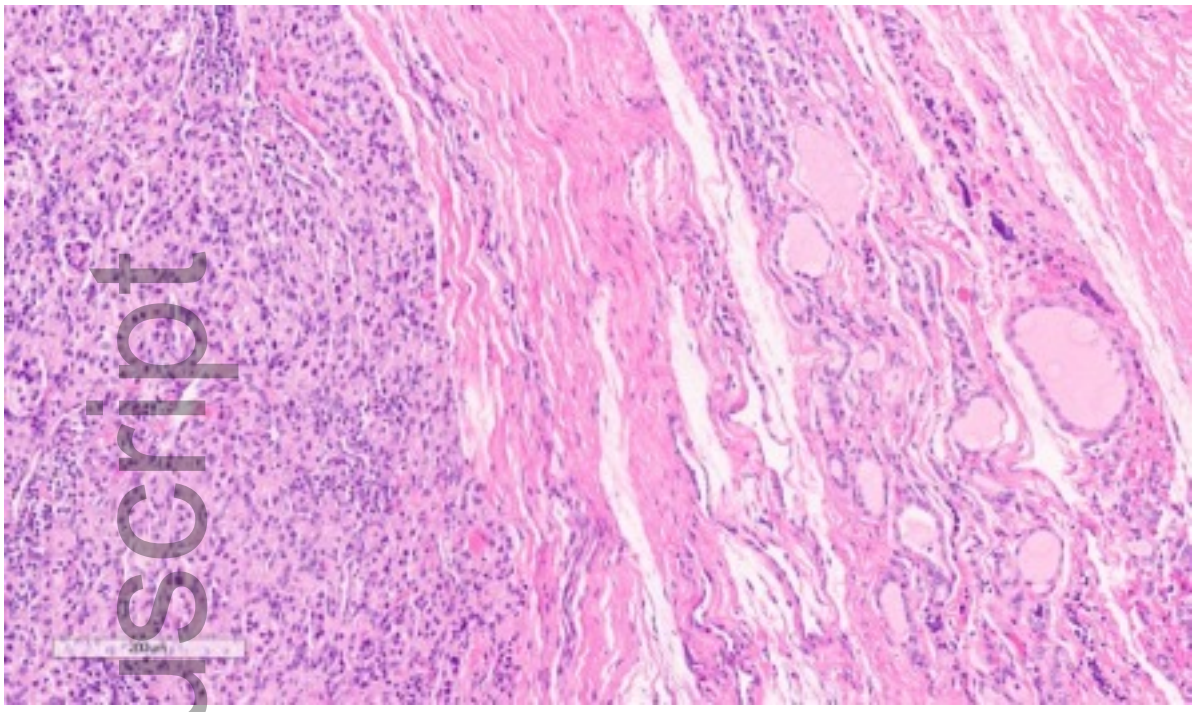

cncy_22404_f5d.tif

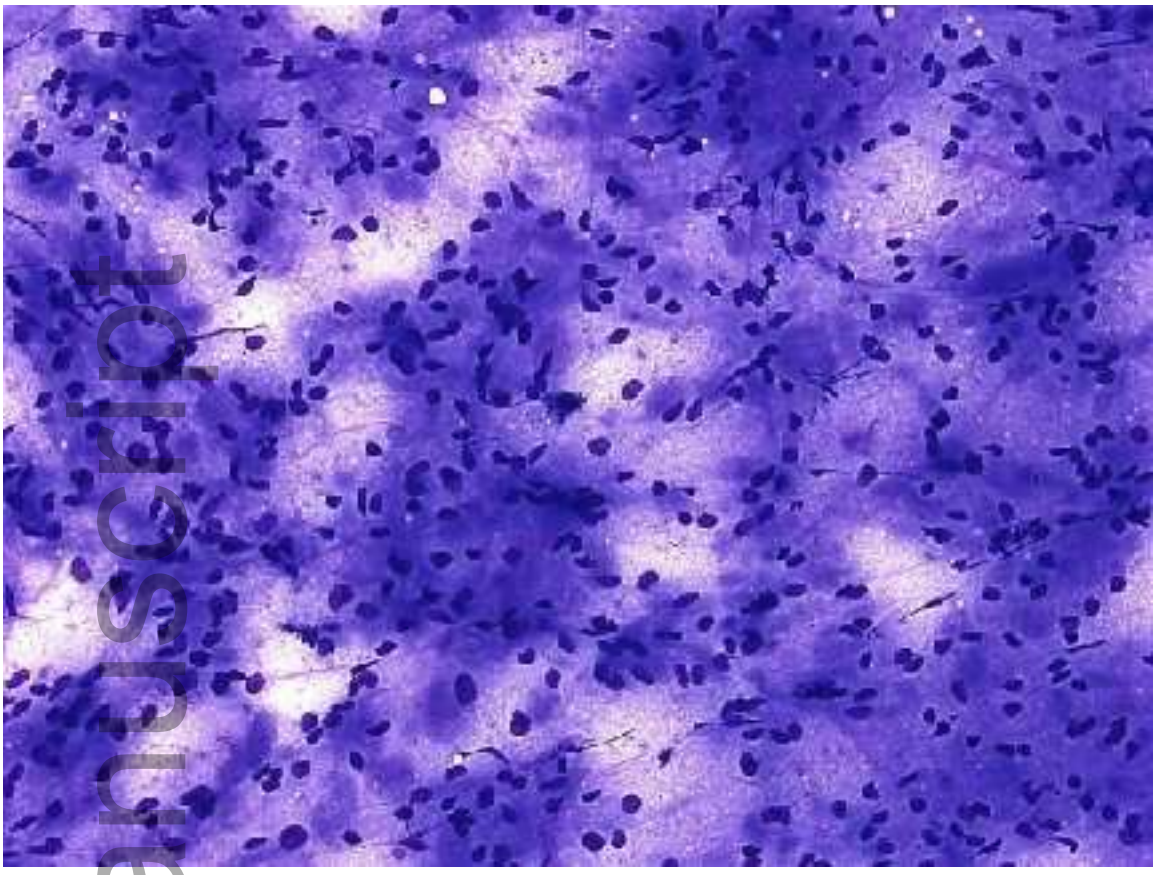

cncy_22404_f6a.tif

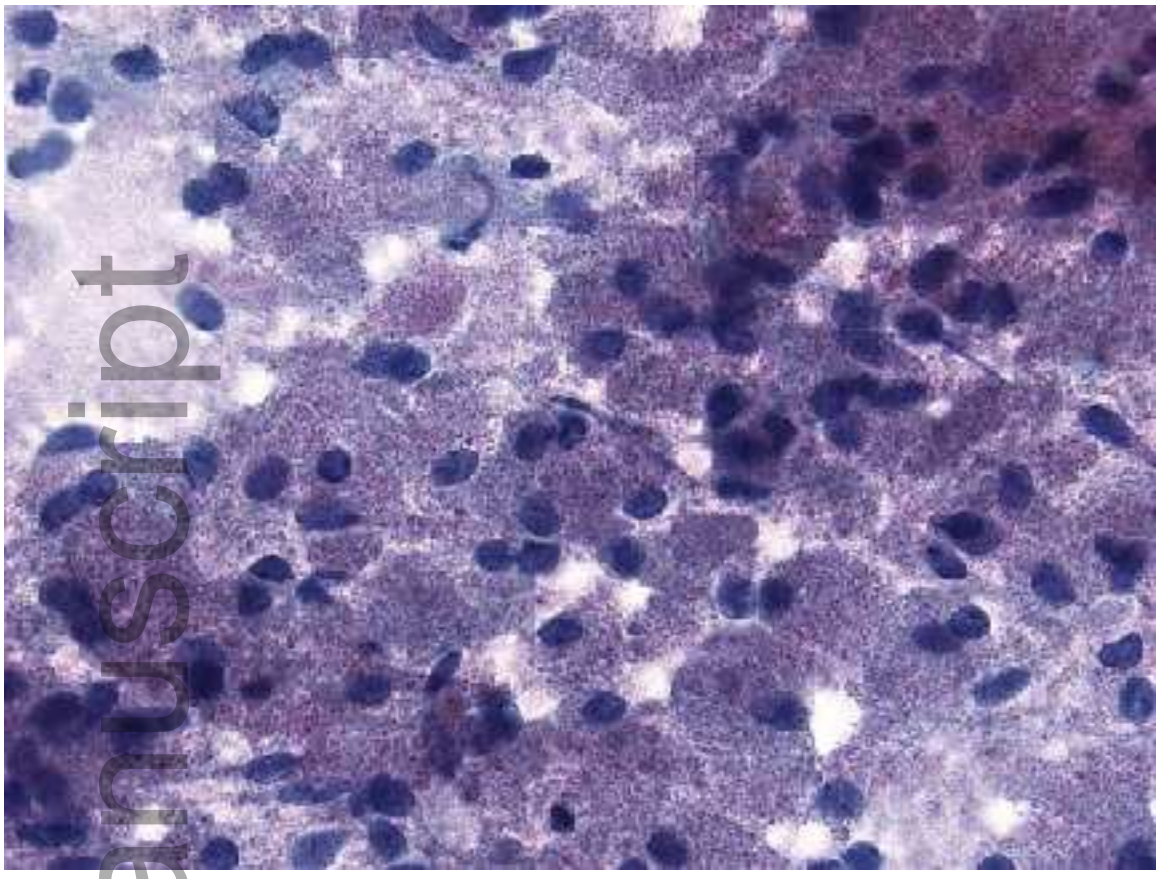

cncy_22404_f6b.tif

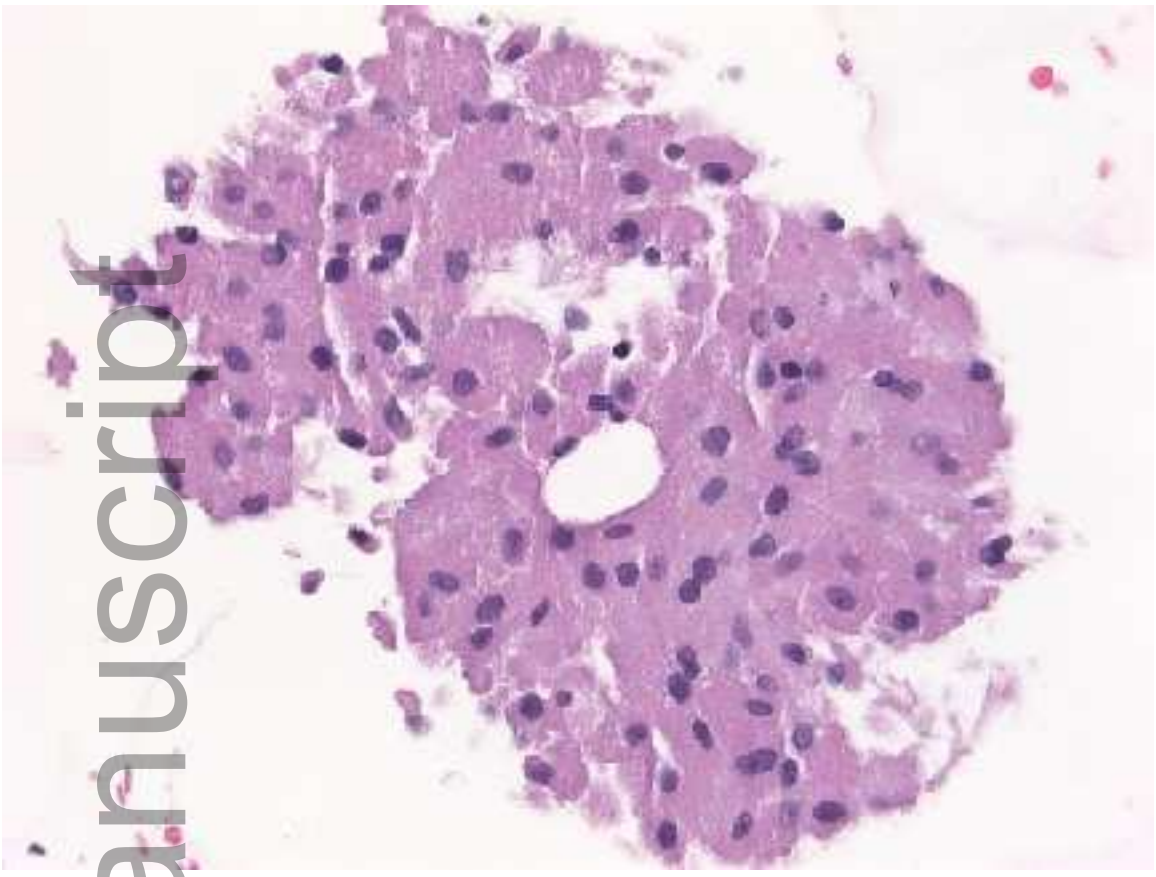

cncy_22404_f6c.tif

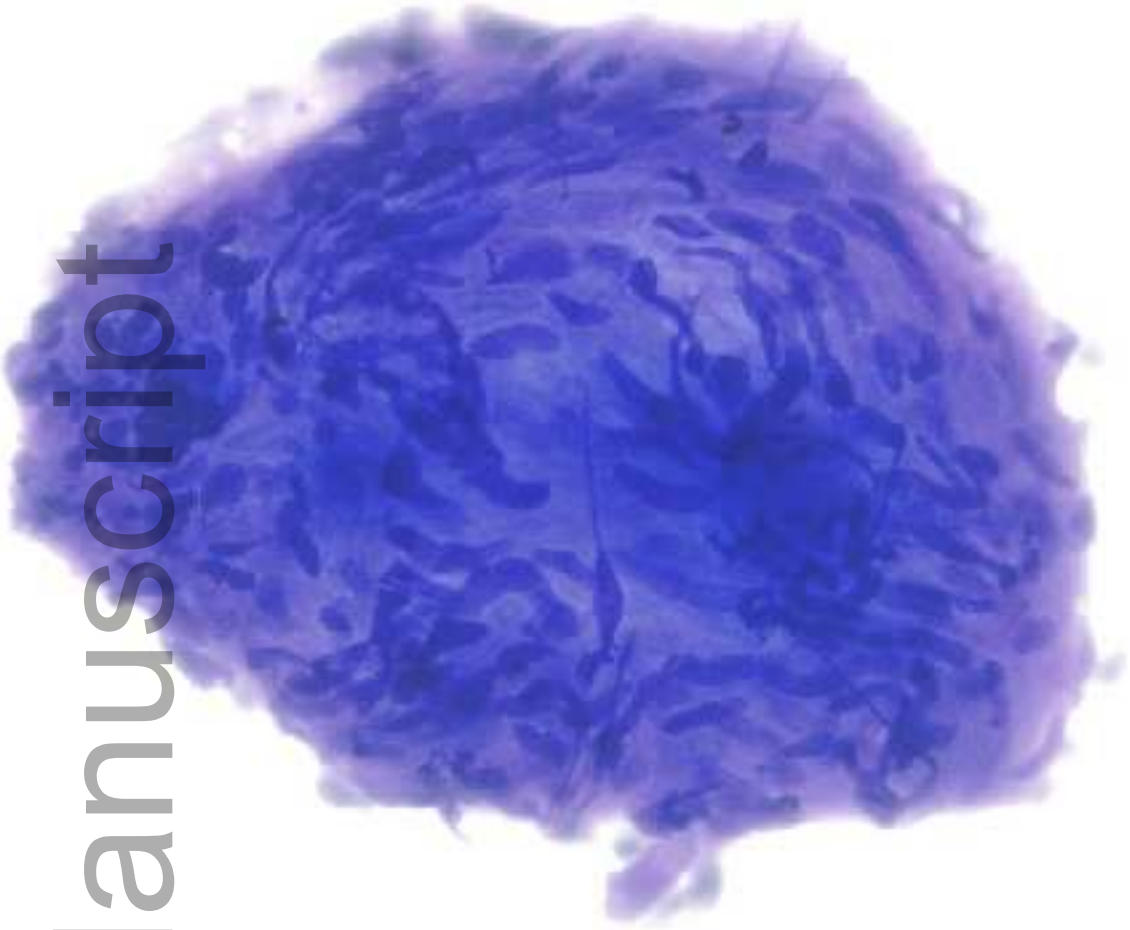

cncy_22404_f7d.tif

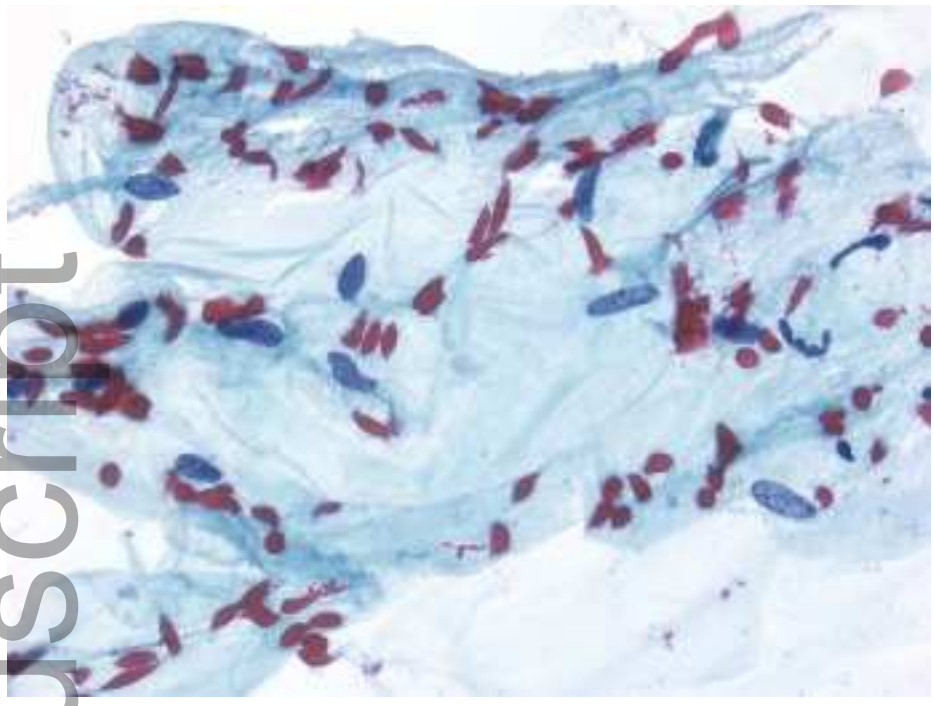

cncy_22404_f8a.tif

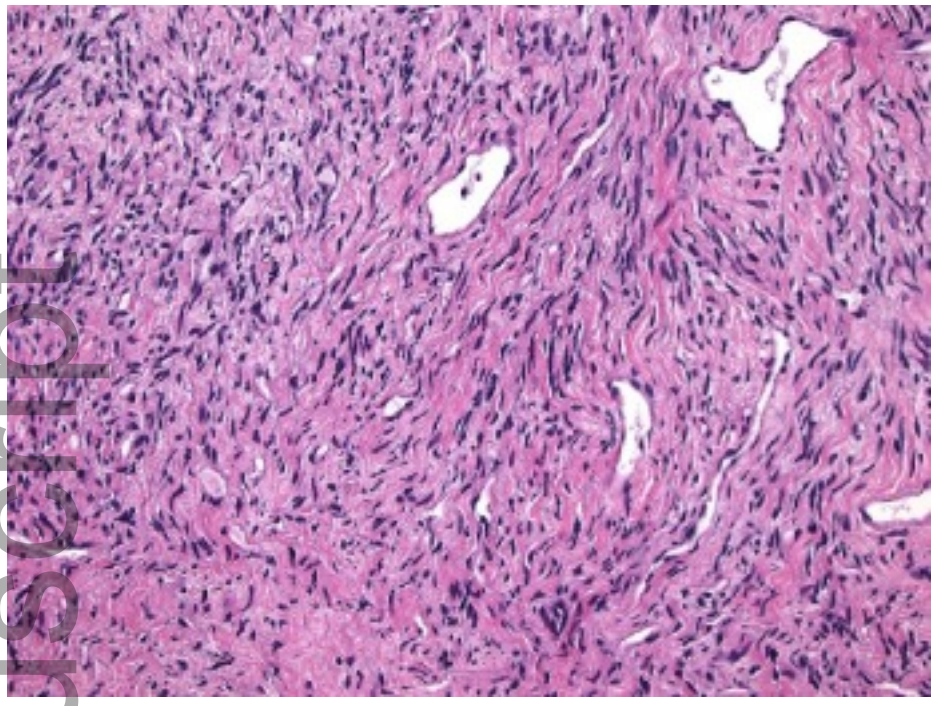

cncy_22404_f8b.tif

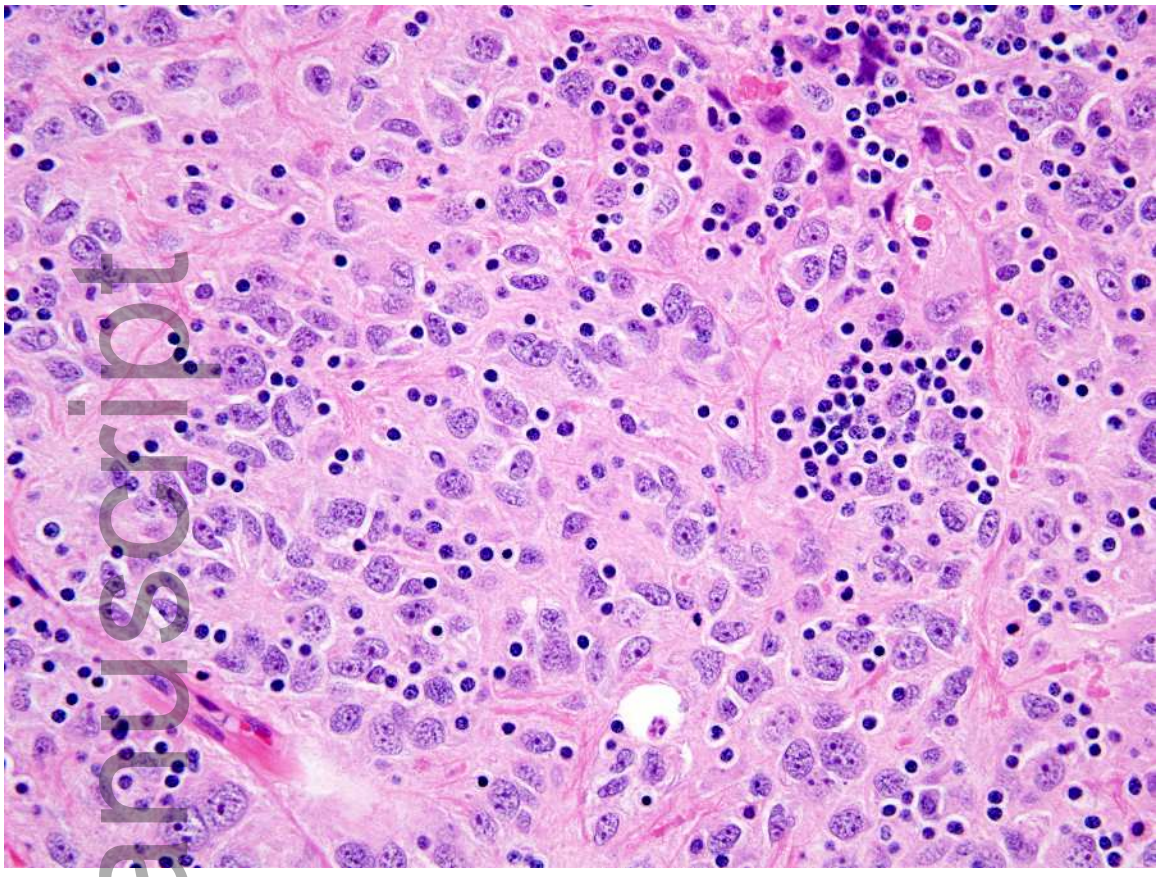

cncy_22404_f9.tif

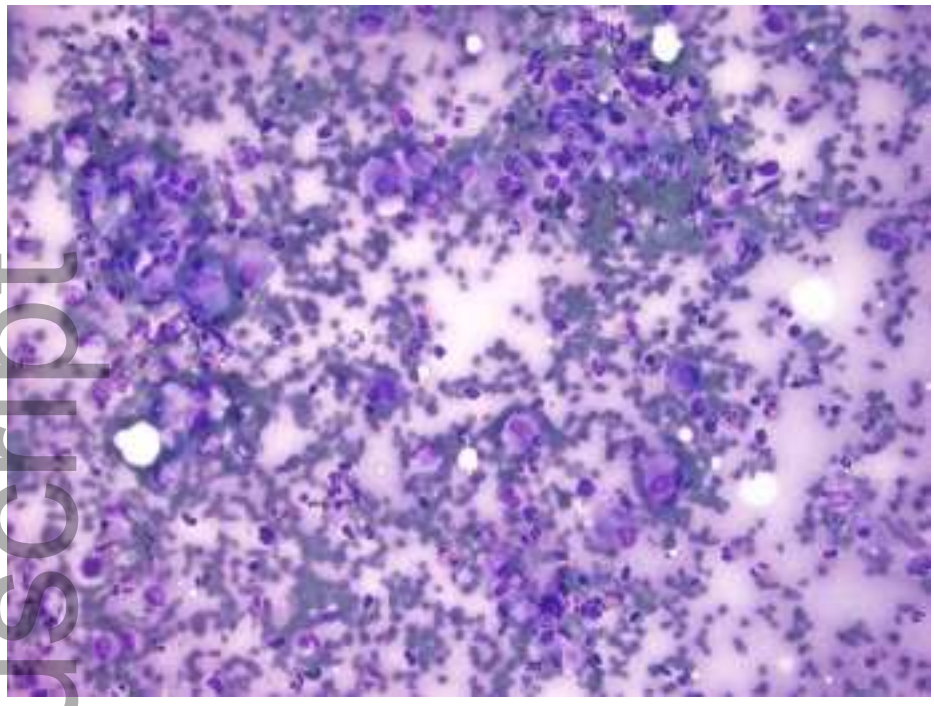

cncy_22404_f10a.tif

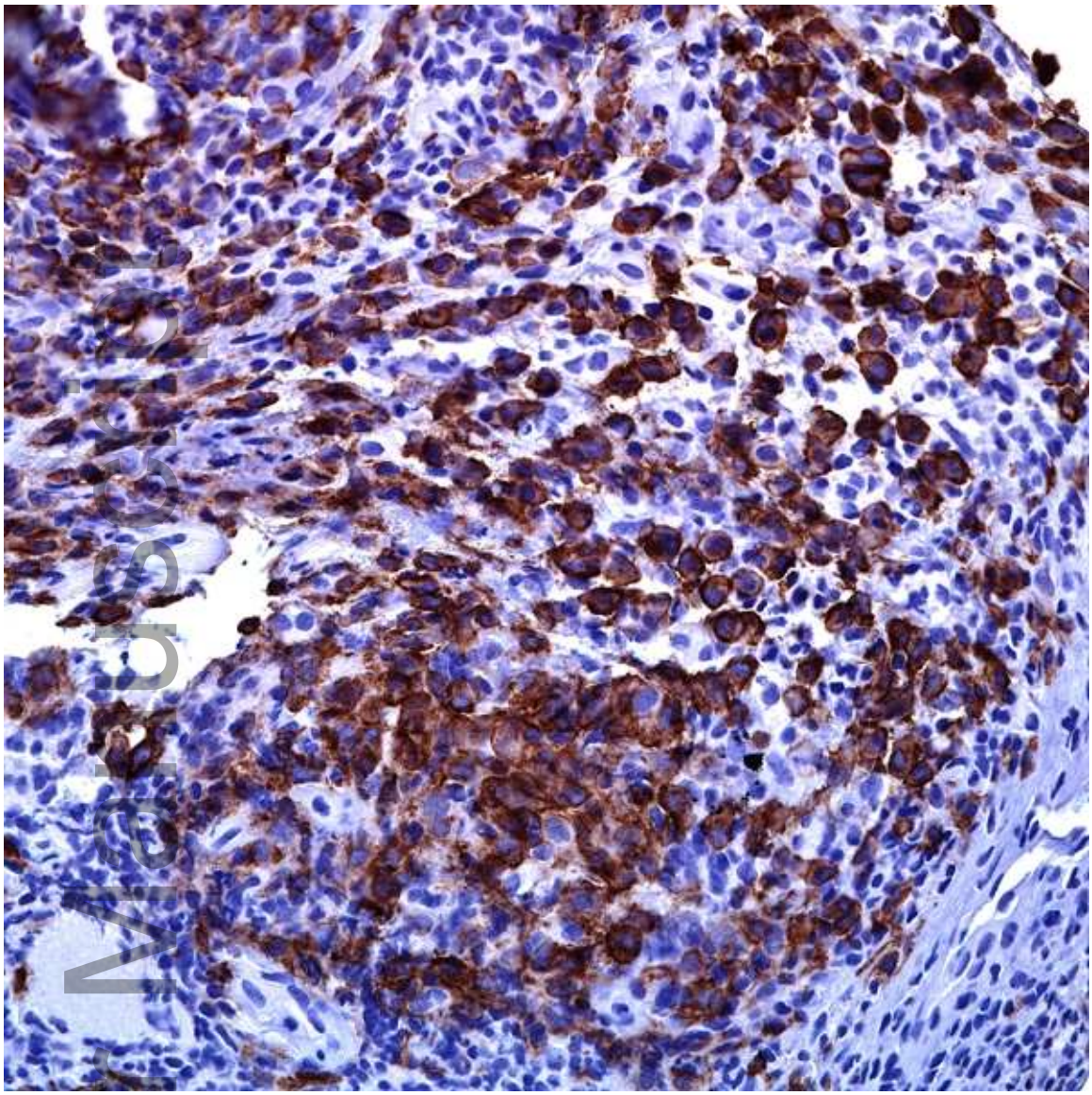

cncy_22404_f10b.tif

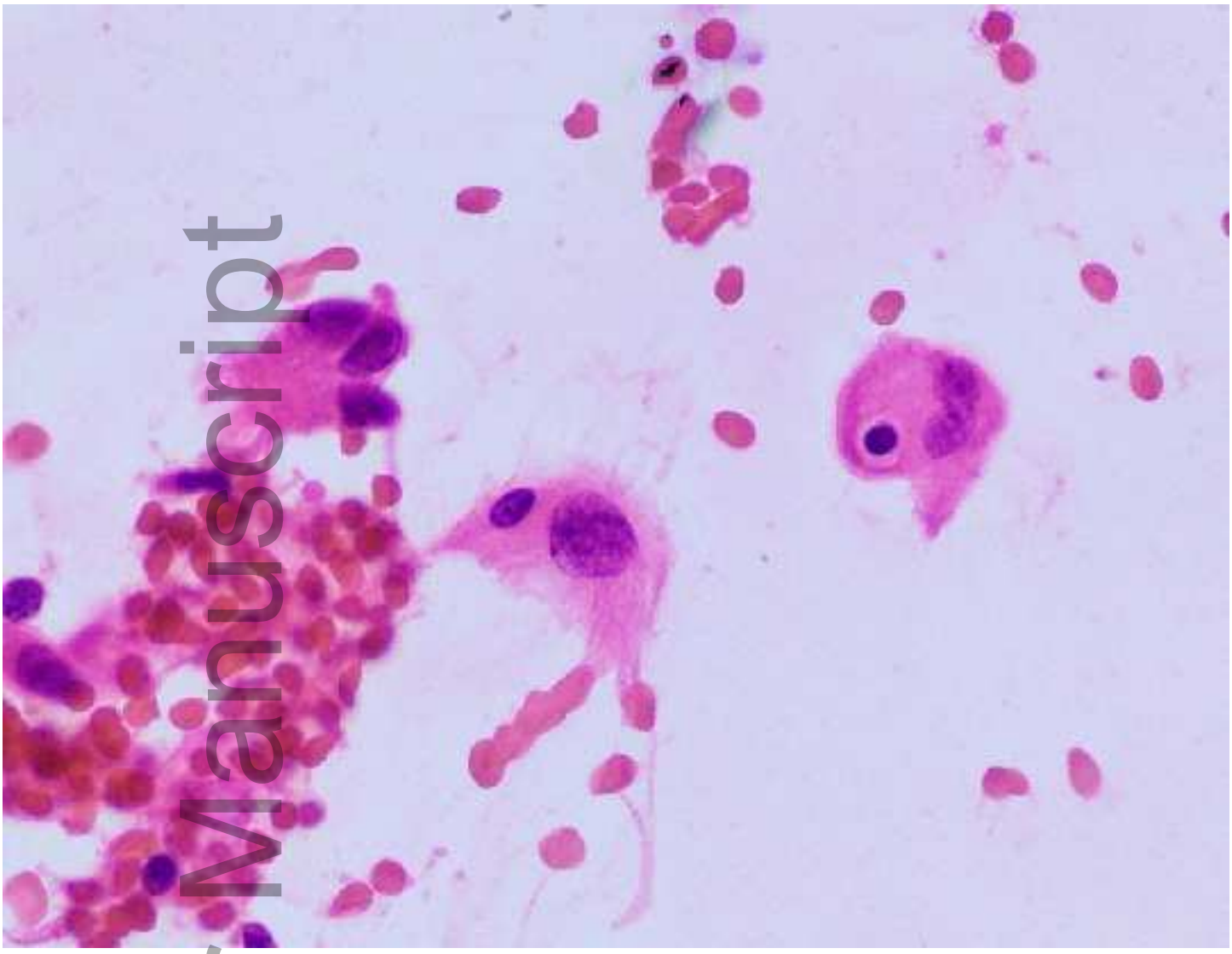

cncy_22404_f11a.tif

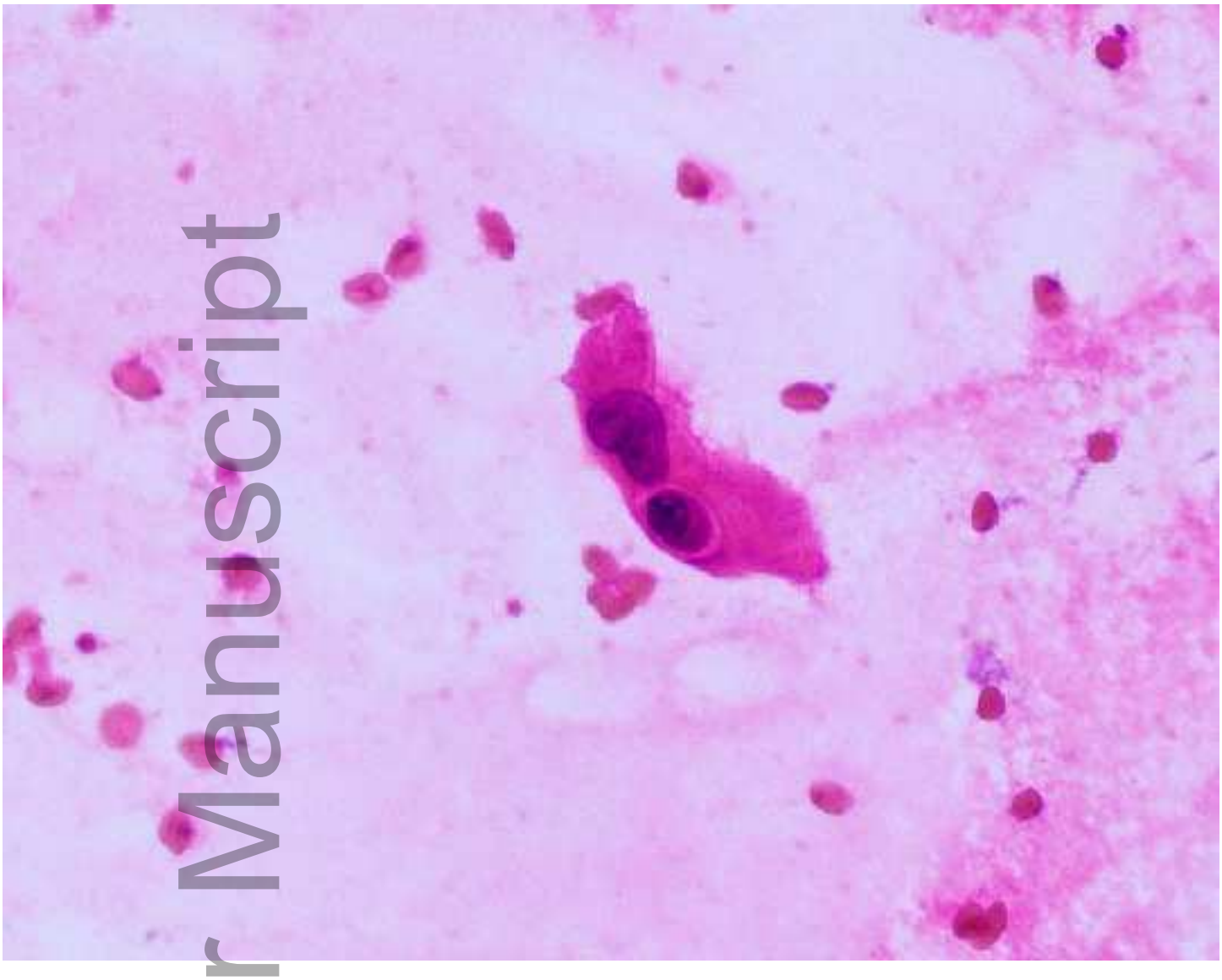

cncy_22404_f11b.tif

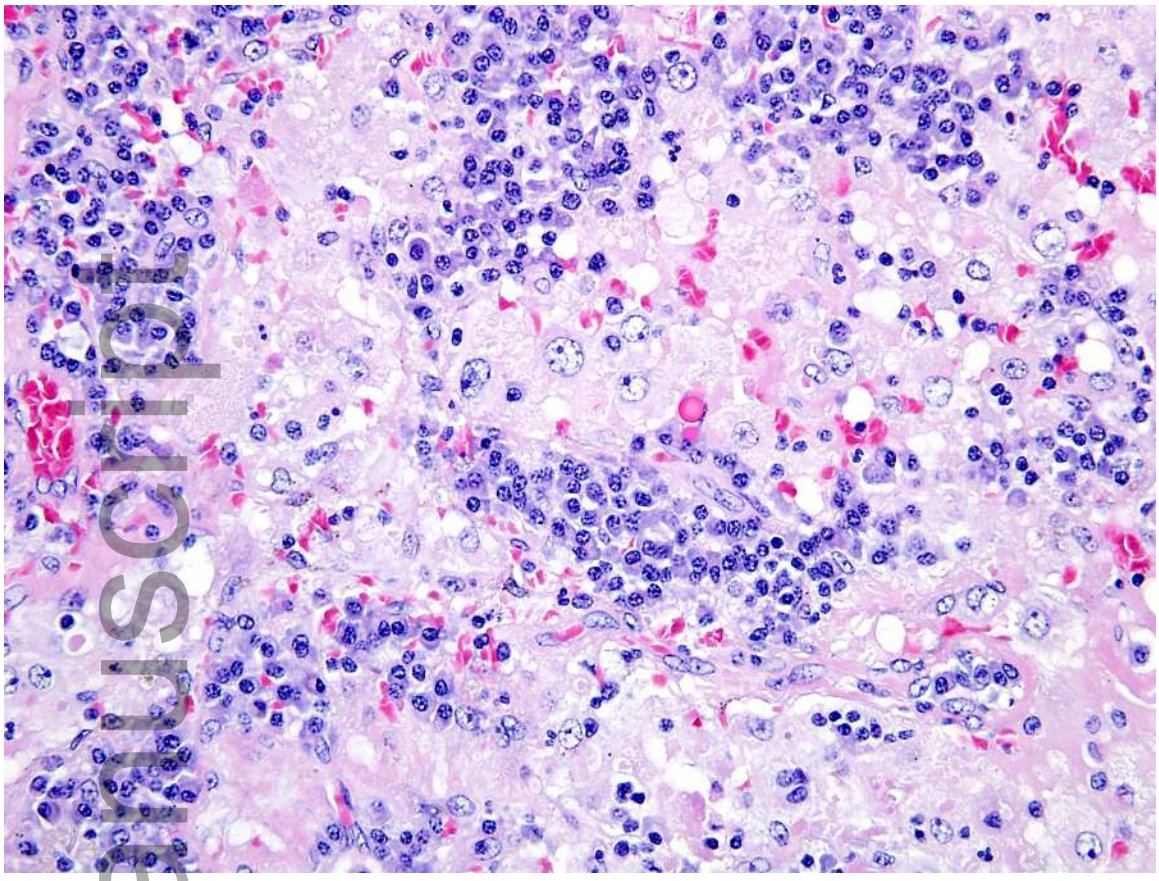

cncy_22404_f11c.tif

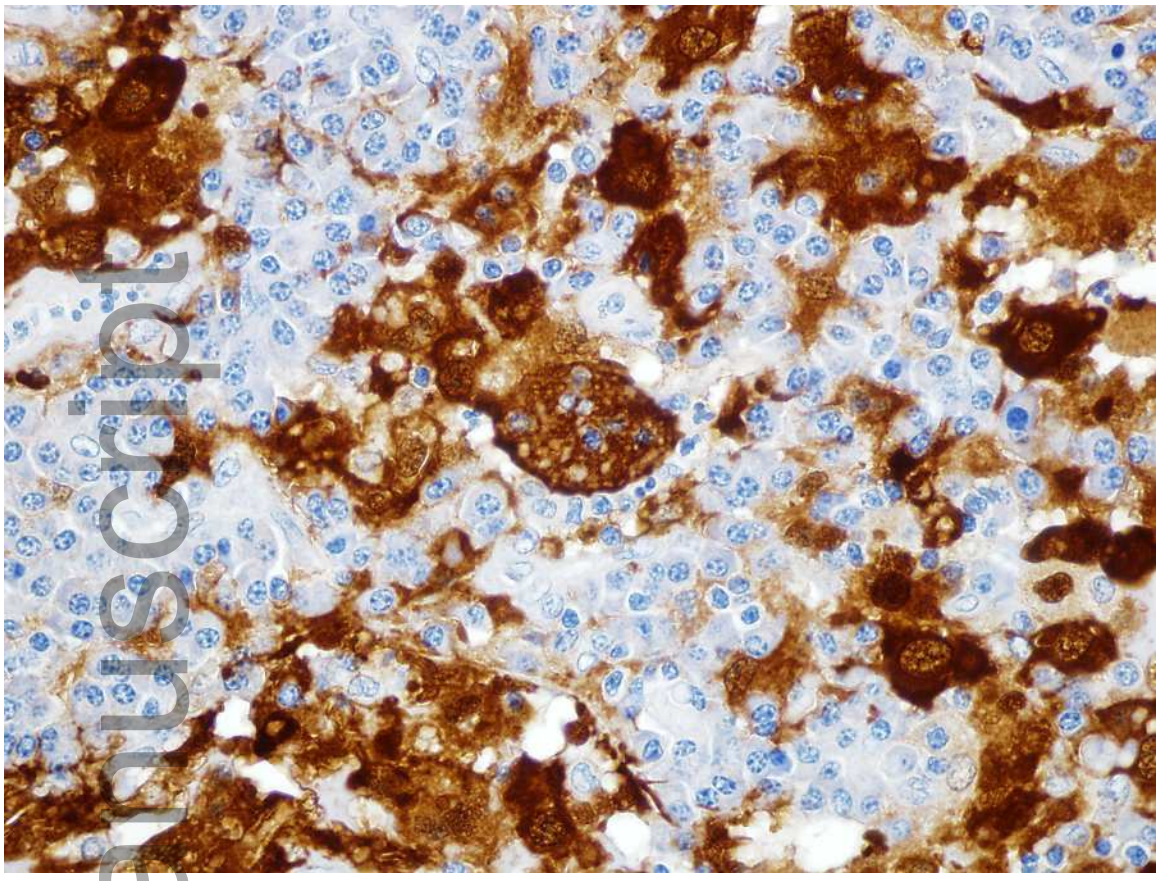

cncy_22404_f11d.tif